JOURNAL OF RESEARCH of the National Bureau of Standards—A. Physics and Chemistry
Vol. 66A, No. 5, September–October 1962

Lattice Frequencies and Rotational Barriers for Inorganic Carbonates and Nitrates From Low Temperature Infrared Spectroscopy

R. A. Schroeder,[1] C. E. Weir, and E. R. Lippincott [2]

(May 29, 1962)

Infrared absorption spectra of inorganic nitrates and carbonates have been obtained on single crystals at room temperature, under liquid nitrogen refrigeration and under liquid helium refrigeration. Diffuse absorption observed in the room temperature spectra between about 1400 cm^{-1} and 700 cm^{-1} is resolved under liquid helium refrigeration into a large number of bands not attributable to fundamentals or combinations of fundamental frequencies of the anions. Almost all of these bands are readily interpreted as summation bands of fundamental frequencies with successive levels of a librating oscillator. The libration is considered to represent a planar torsional oscillation of the anion about the trigonal axis. The librational frequency depends in part on the crystal structure and on the ions. In a given material the librational frequency as determined from successive bands is reasonably constant. In the substances studied the librational frequency varied from about 15 cm^{-1} to 30 cm^{-1}.

Band limits observed in the spectra are interpreted as representing rotational energy barriers. These barrier heights are approximately 200 cm^{-1} with some dependence on the crystal structure and the ions involved. Barrier heights calculated from a cosine potential function agree reasonably well with the observed barriers for the cubic and calcite structures. Similar calculations have not been made for other structures studied because of doubtful assignments or unknown structural details. In particular, spectra of the aragonite structures are remarkable in detail and complexity, and have not been analyzed. However, the details of these and all other spectra studied appear to involve similar phenomena.

1. Introduction

Free rotation of atomic groups in the solid phase was suggested initially by Pauling in 1930 [59] [3]. A number of reports appeared subsequently presenting evidence for free rotation in solids [5,25,32, 39,40,41,65]. In general, the experimental evidence presented consisted chiefly of plausible interpretations of X-ray structure determinations of various solid phases in the ammonium salts and in metal nitrates and carbonates. It was argued that essentially free rotation of the nonspherical ion would be necessary to produce a NaCl-type structure which was required by the X-ray data from these salts. In other structures containing nitrate and carbonate ions free rotation of the ion about the trigonal axis was proposed to satisfy the X-ray data. It has been argued more recently that a disoriented arrangement of the nonspherical ions would also satisfy the diffraction data without the necessity for free rotation [45].

Completely unambiguous evidence of rotation in solids has been sought actively. The question has been pursued with an increasing number of experimental techniques being brought to bear such as X-ray studies [6, 22, 45, 68], specific heat measurements [48], infrared spectroscopy [34, 35, 74, 75], Raman spectroscopy [9, 10, 11, 12, 25, 36, 42, 43, 44, 55, 62, 63, 64], nuclear magnetic resonance [3, 4, 16, 28], and neutron diffraction [18, 31, 49, 50, 53]. In each of these fields the literature is extensive and the references cited are not exhaustive but are confined to the inorganic materials of interest here. Almost without exception, all studies agree that free rotation does not take place at ordinary temperatures. However, they conclude that hindered rotation, i.e., a torsional oscillation or libration does take place with potential barriers sufficiently low that disordering may occur near room temperature. The only exceptions appear to be in NH_4I where there is evidence [61, 72] from heat capacity and infrared data that the NH_4^+ rotates about an N–H–I axis above 75 °K, and in a recent report [18] of free rotation in KCN based on neutron diffraction studies. The present ideas suggest librating ions are able to surmount the barriers at a rate sufficiently great to satisfy the X-ray structure requirements. In effect the findings substantiate the suggestions advanced by Frenkel in 1943 [23] who opposed Pauling's rotation hypothesis and proposed instead torsional oscillation with a finite disordering rate.

Harmonic librations are lattice modes and might be detected by Raman or infrared spectroscopic studies. The frequencies expected for these modes cannot be predicted without knowledge of the potential energy function describing the potential barrier. Although

---

[1] Present address, University of Southwestern Louisiana, Lafayette, La.

[2] Consultant to the Mineral Products Division, National Bureau of Standards. Present address, Dept. of Chemistry, University of Maryland, College Park, Md.

[3] Figures in brackets indicate the literature references at the end of this paper.

the rotational frequencies of the free ion can be calculated readily it is only possible to predict that the frequency of the restricted harmonic librator must be greater than that for the free rotator. Low frequency shifts have been found in the Raman spectra of inorganic solids for which there is independent evidence of anion or cation libration [for example, preceding references on Raman spectra]. Certain Raman lines have been attributed to frequencies arising from harmonic libration modes; however, there is no assurance that these represent the fundamentals rather than overtones or combinations. There is also no conclusive evidence for harmonic libration in the infrared spectra of solids, although Hexter [34, 35] has proposed that certain complex high frequency overtone and combination bands in the 3000 cm^{-1} to 5000 cm^{-1} region of carbonates and nitrates arise from libration combinations. Early reststrahlen studies [51] have shown the existence of low frequency infrared bands whose exact origin is unknown. These bands have been widely attributed to lattice vibrations of an unspecified nature.

This paper will present evidence for libration in the infrared spectra of anhydrous metal nitrates and carbonates. These substances have been the subject of infrared studies since the early work of Schaefer, Bormuth, and Matossi [66] and the spectra are believed to be well understood insofar as the assignments of the six fundamental vibrations of the free nitrate and carbonate ions [30, 33, 38] are concerned. However, the strong overtone and combination bands and their complexity have been the source of recent studies [29, 34, 35]. The very intense and obviously complex band containing the antisymmetric stretching band has also been of concern [52]. Newman and Halford [57, 58] observed in the infrared spectra of crystalline $Pb(NO_3)_2$ and $TlNO_3$ bands that were not attributable to fundamentals of the anions. They were assigned to sum and difference bands of the symmetric stretching vibration and a low lying (30 cm^{-1}) lattice mode. Recently Gross and Shultin [26] studied $Ba(NO_3)_2$ and $Pb(NO_3)_2$ with similar results and succeeded in resolving several combination bands. Both of these studies used low temperatures (liquid nitrogen temperature) to improve the resolution. A careful examination of the pioneering spectra given by Schaefer, Bormuth, and Matossi [66] on the crystalline carbonates shows clear evidence of weak bands in the frequency range containing the fundamentals. In this early work some attempt was made to explain these bands as sum and differences between fundamentals or between fundamentals and lattice frequencies reported from reststrahlen experiments, but with only partial success.

Recent studies in this laboratory of the effect of high pressure on the infrared spectra of crystalline nitrates and carbonates showed the sum and difference modes previously reported in the heavy metal nitrates and produced evidence for additional bands of this type at elevated pressures. These observations motivated a serious study of the combination bands at 1 atm in an attempt to understand the behavior at elevated pressures.

It is obvious that extensive combinations involving sum and difference bands between a lattice fundamental of the order of 30 cm^{-1} and the internal fundamentals of the anion found between 700 cm^{-1} and 1500 cm^{-1} will produce such a complex overlapping band structure as to make analysis extremely difficult. If the spectrum were simplified by removing the difference bands through cooling as suggested by Hornig [38] the fact that 30 cm^{-1} levels are involved would require very low temperatures. Simple calculations showed that at the temperature of liquid nitrogen, large numbers of ions would be in upper states when the levels are spaced 30 cm^{-1} apart. At the temperature of liquid helium, however, almost all of the ions would be in the ground state. This report presents data on the room temperature and on the low temperature—liquid nitrogen and liquid helium temperature—infrared spectra of "thick" (about 0.010 in.) crystals of metal nitrates and carbonates. The spectra are interpreted in terms of librations of the anions.

2. Experimental Method

2.1. Apparatus

Most infrared spectra were recorded on a commercial double-beam spectrometer using NaCl prisms. To permit the use of small thick crystals the spectrometer was equipped with a microfocusing unit employing reflecting optics. This unit was modified for use with the spectrometer and further to permit introduction of the tip of a Dewar into the focal region. The modified unit produced a focal spot 0.060 to 0.080 in. in diameter within a working space 1⅛ in. wide. Approximately 45 to 50 percent of the normal energy was available with the microfocus unit. Only a single unit was available, and this increased the path length of the specimen beam by about 18 in. over the path length of the reference beam. Therefore, complete compensation for water vapor and carbon dioxide was not achieved. Weak bands for these materials appeared in all spectra near 1700 cm^{-1}, 2350 cm^{-1}, and 3500 cm^{-1}. These regions were not of particular interest in the data but caution was exercised in interpreting weak bands near these frequencies.

The overtone and combination region at frequencies above 1700 cm^{-1} was studied on a double beam spectrometer using a grating to provide greater resolution in the higher frequency region. This unit was equipped with a reflecting microfocus unit in both beams to provide for better compensation. Weak bands, particularly in the 3500 cm^{-1} region, indicated incomplete compensation.

The low temperature equipment was constructed to utilize an available commercial Dewar. This was a triple-wall stainless steel unit open at the bottom to permit access to the tip of the innermost liquid container. The central wall comprised a radiation shield that extended well below the liquid reservoir. A specimen holder was fabricated from a ½ in. diam bar of copper. The bar was approximately 2 in. long, threaded at the top end to screw tightly into the tip of the liquid reservoir and machined down at the bottom end to give a flat plate $\frac{1}{2}$ in. square times $\frac{1}{8}$ in. thick. The length of 2 in. was necessary to permit specimens mounted in the flat bottom plate to be positioned in the focal spot of the rather large ellipsodial focusing mirror. The specimens were mounted over holes 0.060 in. in diameter drilled in the flat plate. Five holes were drilled in two rows, the top row containing three holes, the bottom row two. Holes were located $\frac{1}{4}$ in. apart and holes in the two rows were staggered so that a single hole could be brought into the focal spot with no stray radiation through the adjacent holes. Each hole was counterbored from each side of of the plate to a diameter of $\frac{1}{8}$ in. and of such depth that a flat web of copper approximately $\frac{1}{32}$ in. thick remained in the center of the plate. Counterboring permitted entry of the highly convergent cone of radiation and afforded a relatively shallow well in which the crystals were mounted. The Dewar was closed with a brass housing which enclosed the copper bar and was equipped with two NaCl windows located opposite the flat plate on the bottom of the copper bar. Vacuum closure between the housing and the outer wall of the Dewar was accomplished satisfactorily with a rubber O-ring seal. The restricted working space between the ellipsoidal mirrors required miniaturization and although considerable clearance between brass housing and copper bar was provided, it did not prove feasible to extend the radiation shield around the copper bar inside the housing. Attempts to insert such a shield invariably resulted in a thermal short circuit produced by nonuniform contraction of the inner container or the radiation shield assembly on cooling. Some radiation protection was provided by wrapping the copper bar with bright aluminum foil. The Dewar was evacuated through a cutoff valve by means of an oil diffusion pump backed up by a mechanical pump. The complete Dewar assembly was rigidly mounted in a rack equipped with guides and adjusting screws to permit controlled motion in three perpendicular directions. This mount was essential to afford rapid, controlled centering of the small holes in the equally small focal spot.

Five crystals, each covering a single hole, were studied in a single experiment. The small crystals required ($\frac{1}{8}$ in. in diameter) were generally available from reagent bottles or crystal fragments. Crystals were selected for clarity and shape, one reasonably flat surface being required. They were then filed down to fit snugly against the $\frac{1}{32}$ in. web at the bottom of the $\frac{1}{8}$ in. wells, and were cemented into place against the web and the walls of the well with a low temperature resin. All crystals were mounted on the same side of the web and in use this side was turned away from the incident radiation. This arrangement minimized heating of the crystals by unused radiation and eliminated problems arising from absorption by the adhesive. Crystals were checked for thickness while in place by their spectra; if too thick, they were thinned in the center by using water or dilüte acid. In these studies estimated crystal thicknesses ranged from about 0.001 to 0.080 in.

In a given experiment spectra were recorded at room temperature and, following exhaustive evacuation of the Dewar, were recorded at liquid nitrogen temperature. If the runs at liquid nitrogen temperature proved successful, liquid helium was introduced into the Dewar immediately after removing the liquid nitrogen and the final spectra were then recorded. In an ordinary experiment with approximately 1 liter of liquid helium in the Dewar, the rate of boil-off of the helium was sufficiently low to provide cooling for at least 4 hr with the energy input supplied by the spectrometer and the normal environment. This period was more than sufficient to obtain the spectra of the five specimens. Following an experiment the crystals were found to be still firmly cemented in place and, although generally fractured by thermal contraction or the stresses produced by the adhesive, appeared to be in good thermal contact with the copper. Each cooling cycle appeared to produce further fracturing which tended to increase scattering losses and reduce transmission. Thus it was found to be desirable, wherever possible, to obtain all spectra on a single cooling cycle.

In these experiments it was not considered feasible to attempt to measure the temperature of the small crystal specimens. The temperature of the flat copper strip was measured in a typical experiment and with liquid nitrogen in the Dewar a value of 86 °K was obtained while with liquid helium the temperature was found to be 27 °K. These temperatures represented the temperature of the copper bar at a point as far from the coolant as possible, measured with a gold-cobalt alloy-copper thermocouple [54]. The actual temperature of a crystal might have been higher because of the energy flux from the focal spot, with the temperature being determined by the absorption, the specific heat, the thermal conductivity of crystal and cement, and the thermal barriers between crystal and cement and copper, or lower because of the thermal energy introduced by the thermocouple leads. On the other hand the thermal path was very short and the crystal was nearly surrounded by the cold copper strip. In several spectra of interest the difference band between the symmetric stretching mode and a level of the order of 30 cm^{-1} was identified. This band in effect represented a thermometer built into the spectrum and observations showed that the difference band, although somewhat reduced in intensity, was still very prominent at the temperature of liquid nitrogen. With liquid helium in the Dewar, however, the difference band was effectively missing. This result may be taken as evidence that the temperature of the crystal was sufficiently low to remove all difference modes involving energies of 30 cm^{-1} or more. The removal of difference bands was the primary objective of cooling and the result showed that, irrespective of the absolute temperature of the crystal, the resulting spectra could be interpreted in terms of the fundamentals and their summation bands only. In tabulating the spectra the temperatures will be described as liquid nitrogen temperature and liquid helium temperature with the clear understanding that the temperatures of the crystals may differ appreciably from the boiling temperatures of these liquids.

2.2. Materials Studied

The following nitrates were studied: $NaNO_3$, KNO_3, $RbNO_3$, $CsNO_3$, $TlNO_3$, $AgNO_3$, $Sr(NO_3)_2$, $Ba(NO_3)_2$, and $Pb(NO_3)_2$. Of these all except $RbNO_3$, $CsNO_3$, and $TlNO_3$ were reagent grade chemicals of high purity. These three materials were recrystallized from aqueous solution at 55 °C to effect further purification and to prepare suitable crystals. This technique was used by Newman and Halford [58] to prepare large $TlNO_3$ crystals. Suitable crystals for the other materials were obtained from the substances as received.

The following carbonates were studied: $MgCO_3$, $CaCO_3$, $SrCO_3$, $BaCO_3$, $PbCO_3$, $FeCO_3$, and $MnCO_3$. These were all natural minerals obtained in large crystals. The materials and their sources are as follows:

$MgCO_3$—magnesite—origin uncertain (large clear crystals)
$CaCO_3$—calcite—Brazil (large clear crystals)
$SrCO_3$ — strontianite — Argyll, Scotland (large translucent crystals)
$BaCO_3$ — witherite — Lancashire, England (large translucent crystals)
$PbCO_3$—cerrusite—Southwest Africa (large clear crystals)
$FeCO_3$—siderite—Roxbury, Conn. (opaque masses, obviously impure)
$MnCO_3$—rhodochrosite—Kusatuni Kaga, Japan (opaque—large crystals)
$CaCO_3$—aragonite—Cianciano, Sicily (large translucent crystal).

Spectrochemical analyses were performed on all carbonates except the $CaCO_3$ (aragonite). Aside from trace impurities the following metallic impurities were found in quantities up to a maximum of 1 percent. $MgCO_3$-Fe; $CaCO_3$ (calcite)—none; $SrCO_3$-Ca; $BaCO_3$-Sr; $PbCO_3$—none; $MnCO_3$-Ca,Fe, Mg; $FeCO_3$-Mg,Mn,Si. The impurities except in the cases of $MnCO_3$ and $FeCO_3$ appear to be of negligible importance. Inspection of the infrared spectra indicates no evidence for the strongest fundamentals of the major contaminant.

The materials studied fall into the following five classes at room temperature.

(1) calcite type—space group D^6_{3d}-$NaNO_3$, $MgCO_3$, $CaCO_3$ (calcite), $MnCO_3$, and $FeCO_3$ [71];
(2) aragonite type—space group V^{16}_h-KNO_3, $CaCO_3$ (aragonite), $SrCO_3$, $BaCO_3$, and $PbCO_3$ [7, 8, 17, 71, 79];
(3) hexagonal—space group C^4_{6v}-$CsNO_3$, $RbNO_3$ [19, 20, 21, 60, 76];
(4) orthorhombic — space group uncertain — $TlNO_3$, $AgNO_3$ [37, 71];
(5) cubic—space group T^6_h-$Sr(NO_3)_2$, $Ba(NO_3)_2$, $Pb(NO_3)_2$ [71].

Specific heat data are available for most of these substances between room temperature and lower temperatures which range from 55 to 13 °K with no reports of any structural changes. $CaCO_3$ (calcite), $CaCO_3$ (aragonite), $SrCO_3$, and $BaCO_3$ were studied by Anderson down to 55 °K [1]. Anderson also has reported data down to 55 °K for $MgCO_3$, $PbCO_3$, $MnCO_3$, and $FeCO_3$ [2]. The data on $CaCO_3$ (aragonite) have been extended down to 23 °K by Gunther [27] with no observed transitions. Latimer and Ahlberg have studied $Ba(NO_3)_2$ [46] and $TlNO_3$ [47] down to about 16 °K while Nernst and Schwers [56] have reported data on $CaCO_3$ (calcite) to a temperature of 22 °K. Shomate and Kelley [67] investigated $Ba(NO_3)_2$ to 53 °K and similar data were given to 13 °K for $AgNO_3$ by Smith, Brown, and Pitzer [69]. Finally, data down to 15 °K were obtained by Southard and Nelson for KNO_3 and $NaNO_3$ [70]. In no case were any irregularities in the specific heat curves observed, therefore, no transitions are known to occur between room temperature and the temperatures given. These temperatures may be above the lowest temperature to which the materials were subjected in these studies; however, the specific heat data assure that no transitions occur in the major portion of the temperature range. Low temperature data do not appear to be available for $Sr(NO_3)_2$, $Pb(NO_3)_2$, $RbNO_3$, and $CsNO_3$. By analogy with $Ba(NO_3)_2$ it would be expected that $Sr(NO_3)_2$ would exhibit a regular low temperature behavior. It would appear much less certain that $Pb(NO_3)_2$ would behave similarly. The $RbNO_3$ and $CsNO_3$ represent different systems and to resolve the question low temperature X-ray diffraction patterns were obtained on $RbNO_3$ and $CsNO_3$ to 77 °K. The results showed that no structural changes occurred between room temperature and 77 °K. Behavior at temperatures below 77 °K was not studied.

2.3. Polarization and Orientation Effects

The infrared beam underwent at least three reflections in the process of being focused on the crystal studied. Therefore, some uncertainty existed concerning the polarization of the incident beam. To provide a partial answer to the experimental effects to be expected, two specimens from a single crystal of calcite were studied, one cut parallel and the other cut perpendicular to the optic axis. The absorption spectra of these crystals are shown in figure 1. The spectra are displaced vertically to eliminate overlapping. It will be noted that the spectra are similar. Although some major differences in relative intensity are observed in the two spectra, both crystals show essentially the same absorption bands. It is concluded, therefore, that the degree of polarization of the beam is so small that essentially the same absorption spectrum will be shown by randomly oriented, anisotropic crystals.

3. Results and Discussion

3.1. Method of Presentation

There are a large number of spectra to be presented and discussed and the following pro-

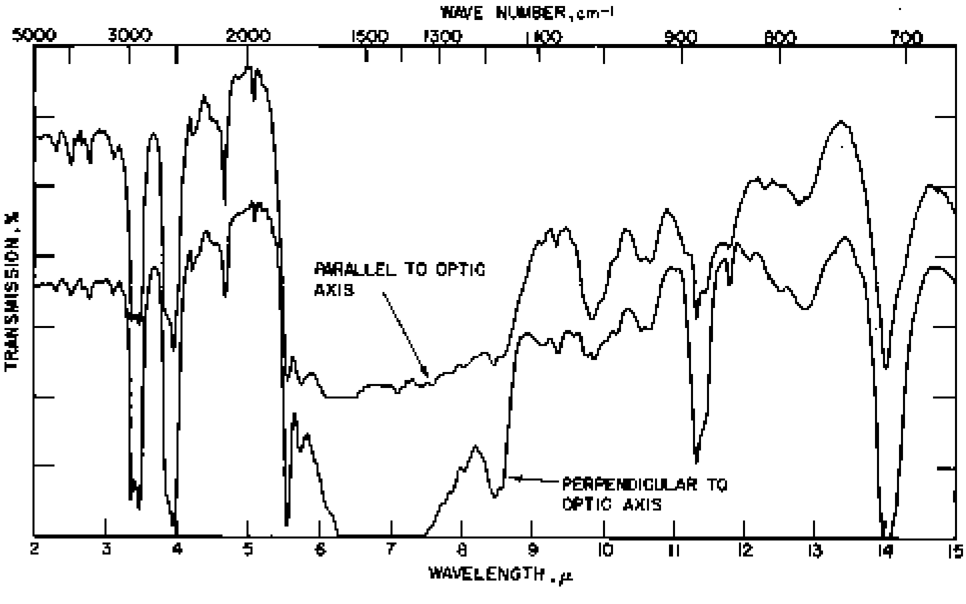

FIGURE 1. *Infrared absorption spectra of calcite crystals of different orientations.*

cedure is employed: (a) The spectra are subdivided with respect to crystal structure because there appear to be good correlations within a given structure. (b) Spectra are shown for each material studied. For each crystal type except the aragonite type at least one spectrum is shown on an enlarged scale for each of the three temperatures studied. These spectra are given in the same figure but displaced vertically. For other materials of the same crystal type two spectra on a small scale are shown, one at room temperature, and the other at liquid helium temperature. These spectra are drawn on the same figure but displaced vertically. (c) The discussion will also be divided, first according to the vibrations of interest. These sections are then further subdivided according to crystal structure. The major discussion will consist of three parts: first, the fundamentals; second, librations; and third, fundamental overtones and combinations.

3.2. Fundamental Internal Frequencies

A discussion of the fundamental internal frequencies for the carbonate and nitrate ions will be given before any additional features of the spectrum are analyzed in terms of lattice modes or combinations. This analysis may be carried out to three stages of approximation for the selection rules applicable to possible infrared transitions. First, the symmetry of the free ion may be assumed, ignoring any effects due to the crystal field symmetry. This assumption would not be expected to be a valid approximation to the actual situation. Second, the site group approximation may be used in which the selection rules for the ions are derived from the symmetry of the site which they occupy in the crystal lattice. In effect the ion is considered as if it were an independent entity possessing the symmetry of the lattice site. This treatment will predict some effects arising from the crystal field symmetry but will not adequately describe those effects due to the interaction of a given ion with its neighbors. Finally the factor group analysis may be considered. This treatment considers the vibrations of the crystal as arising from the motion of the *m* atoms in the unit cell to give 3*m*-3 fundamentals (including both internal and lattice modes). The selection rules are derived from the factor group symmetry which is isomorphous with the space group symmetry. The factor group analysis will differ from the site group analysis in that coupling of vibrations between ions in different sites is included. Vibrations may show higher degeneracy, may become inactive, or may be repeated several times compared to the results of the site group approximation.

a. Free Ion Approximation

Free carbonate and nitrate ions are classified in the point group D_{3h}. Table 1 gives the spectral activity, symmetry species, types of internal frequencies, and the lattice modes derived from transla-

TABLE 1. *Spectral activity for nitrate and carbonate ions of symmetry* D_{3h}

Species	Activity	Internal mode	Lattice modes derivable from translation or rotation
A_1'	Raman	ν_1	
A_1''			
A_2'			$L(R_z)$
A_2''	I.R.	ν_2	$L(T_z)$
E'	I.R., Raman	ν_3, ν_4	$L(T_x,T_y)$
E''	Raman		$L(R_x,R_y)$

I.R. —infrared active; R—Raman active.
L(T)—lattice mode derivable from translation along *x*, *y*, *z*, axis.
L(R)—lattice mode derivable from rotation about *x*, *y*, *z*, axis.
ν_1 —symmetric stretch; ν_2—out-of-plane bend; ν_3—degenerate antisymmetric stretch; ν_4—degenerate in-plane bend.

tions and rotations of the free ion. For the free ion, the active fundamentals and their approximate positions are: the out-of-plane bending (ν_2) observed generally near 850 cm^{-1}; the degenerate antisymmetric stretching (ν_3) which is usually very intense and observed in the 1400 cm^{-1} to 1500 cm^{-1} region; and the degenerate in-plane bending (ν_4) usually found near 720 cm^{-1}. The symmetric stretching mode (ν_1) is inactive in the infrared for the free ion approximation but is expected to have a frequency near 1060 cm^{-1}. Translations of the free ion would be infrared active (species A_2'' and E') but the modes derived from rotations of the free ion would be inactive in the infrared spectrum. The frequencies of the lattice modes would be expected to be less than 500 cm^{-1} and, therefore, unobserved in the present study. However, combinations of these modes with fundamental frequencies would be infrared active and might be observed. Combinations of fundamentals with a number of other lattice modes would be restricted by the D_{3h} symmetry.

Crystals with the calcite, cubic, hexagonal, and orthorhombic structures show spectra conforming reasonably well with the predictions of the free-ion selection rules insofar as the fundamental internal frequencies are concerned. ν_2 and ν_4 are always observed in the expected positions although ν_4 is occasionally weak in some of the nitrates. ν_3 is always observed but with such great intensity that it is not possible to determine whether it is a single or multiple band or even to locate its position with reliability. The symmetric stretching band ν_1 is usually not observed as expected or when present is generally weak. The free-ion model must be rejected because it does not adequately describe the complex spectra of the aragonite crystals shown in figures 9 to 15 nor does it permit sufficient flexibility in the selection rules for combinations between internal and lattice modes to explain the elaborate band structure observed in most specta. For example the D_{3h} selection rules predict that combinations of ν_1 with the lattice libration frequency derived from rotation in species A_2' should be inactive. For reasons to be discussed later a whole series of such bands are believed to be present in the spectra.

b. Site Group Approximation

The selection rules for the various crystal structures in the site group approximation may be obtained from the space group symmetry and the tables given by Halford [30] showing the various sites for each space group. In the calcite type crystals of space group D_{3d}^6 containing 2 molecules per unit cell, the anions occupy sites of D_3 symmetry and the cation's sites of symmetry C_{3i}. In the cubic structures of space group T_h^6 containing 4 molecules per unit cell the anions must lie on sites with symmetry C_3 and the cations on sites of symmetry C_{3i}. Similarly in the aragonite structures of symmetry V_h^{16} with 4 molecules per unit cell both anions and cations occupy sites of symmetry C_s. The hexagonal and orthorhombic crystals will not be discussed because of uncertainties concerning the space groups. The results of the site group approximation for the selection rules are given in table 2.

TABLE 2. *Spectral activity for nitrate and carbonate ions in calcite, aragonite, and cubic structures for the site group approximation*

Calcite structure (site symmetry D_3)

Species	Activity	Internal mode	Lattice mode for anion*
A_1	Raman	ν_1	
A_2	I.R.	ν_2	L(T), L(R)
E	I.R., Raman	ν_3, ν_4	L(T), L(R)

* There are 3 lattice modes of translational origin associated with the cations on sites C_{3i} which are infrared active.

Aragonite structures (site symmetry C_s)

Species	Activity	Internal mode	Lattice mode for anion*
A'	I.R., Raman	ν_1, ν_3, ν_4	2L(T), L(R)
A''	I.R., Raman	ν_2, ν_3, ν_4	L(T), 2L(R)

* There are 3 lattice modes for the cations on sites of symmetry C_s which are active in both infrared and Raman.

Cubic structures (site symmetry C_3)

Species	Activity	Internal mode	Lattice mode for anion*
A	I.R., Raman	ν_1, ν_2	L(T), L(R)
E	I.R., Raman	ν_3, ν_4	L(T), L(R)

* There are 3 lattice modes associated with the cations on sites of symmetry C_{3i} which are inactive in the Raman but active in the infrared spectrum (species A_u and E_{1u}).

Calcite type structures. In the calcite type crystals the selection rules require that ν_2 (species A_2) and ν_3 and ν_4 (species E) are infrared active while ν_1 remains infrared inactive. This prediction agrees with the observed fundamentals but again the selection rules are too restrictive and fail to account for the large number of sum and difference modes believed to be due to lattice modes. As an example, lattice modes of rotational or translational origin in species A_2 would be expected to give a series of combination bands with every other band forbidden by the selection rules. This is not believed to be the case.

Aragonite type structures. In these structures the site symmetry C_s yields selection rules requiring the degenerate stretching and bending modes, ν_3 and ν_4, to be split and the symmetric stretching mode, ν_1, to be active in the infrared spectrum. The out-of-plane bending ν_2 remains active. The low temperature spectra show that ν_3 is split (for example, see spectrum of $SrCO_3$). However, there appear to be at least three components of ν_3 in $SrCO_3$. This does not agree with the selection rules which predict two components only. Similarly, ν_1 is active as predicted but in addition at least one other component of ν_1 appears to be present which is unaccounted for. Considerations of a similar nature arise regarding ν_2 and ν_4.

Cubic structures. With the site symmetry C_3 the selection rules predict that in addition to ν_2 (species A) and ν_3 and ν_4 (species E) that ν_1 (species A) should also be infrared active. Spectra for the cubic crystals show a very weak band in this region which may represent the ν_1 vibration.

It is clear that while the site group approximation gives results which are in better agreement with the observations than the free ion approximation, the apparent discrepancies between prediction and observations in the aragonite structures makes the validity of the approximation questionable. The applicability of this treatment has been discussed previously [13] and it has been pointed out that the site group approximation is less applicable to ionic crystals than molecular crystals because of the much stronger coupling in ionic lattices.

c. Factor Group Approximation

Selection rules for the calcite, aragonite, and cubic crystal types under the factor group approximation are given in table 3. The internal and lattice frequencies are classified with regard to their respective symmetry species.

Table 3.—*Factor group selection rules for the calcite, aragonite and cubic structures*

Species	Activity	Internal mode	Lattice modes
Calcite structure-space group D_{3d}^6; 2 molecules/unit cell; total frequencies—27			
A_{1g}	Raman	ν_1	1
A_{1u}		ν_2	1
A_{2u}	I.R.	ν_2	2
A_{2g}		ν_1	1
E_u	I.R.	ν_3, ν_4	3
E_g	Raman	ν_3, ν_4	2
Aragonite structure-space group V_h^{16}; 4 molecules/unit cell; total frequencies—57			
A_g	Raman	$\nu_1, \nu_2, \nu_3, \nu_4$	5
A_u		ν_3, ν_4	4
B_{1g}	Raman	ν_3, ν_4	4
B_{1u}	I.R.	$\nu_1, \nu_2, \nu_3, \nu_4$	4
B_{2g}	Raman	$\nu_1, \nu_2, \nu_3, \nu_4$	5
B_{2u}	I.R.	ν_3, ν_4	3
B_{3g}	Raman	ν_3, ν_4	4
B_{3u}	I.R.	$\nu_1, \nu_2, \nu_3, \nu_4$	4
Cubic structure-space group T^{1}; 4 molecules/unit cell; total frequencies—105			
A_g	Raman	ν_1, ν_2	2
A_u		ν_1, ν_2	3
E_g	Raman	ν_3, ν_4	2
E_u		ν_3, ν_4	3
F_g	Raman	$\nu_1, \nu_2, \nu_3, \nu_3, \nu_4, \nu_4$	6
F_u	I.R.	$\nu_1, \nu_2, \nu_3, \nu_3, \nu_4, \nu_4$	8

Calcite type structures. For calcite structures, the active modes in the infrared are ν_2 (species A_{2u}), ν_3 (species E_{1u}), and ν_4 (species E_{1u}). The symmetric stretch, ν_1, is again inactive. As before, the predictions agree well with the observed fundamentals. There are now effectively no selection rules governing combinations between fundamentals and lattice modes [78].

Aragonite type structures. In these crystals the selection rules predict that three nondegenerate components of ν_3 and ν_4 (species B_{1u}, B_{2u}, and B_{3u}) should result from the splitting of the degenerate stretching and bending modes of the free ion. In the $SrCO_3$ spectrum three such bands can be observed at 1362, 1445, and 1522 cm^{-1}. These are sharp, strong, bands and may be taken to represent the three components of ν_3. The very strong broad band near 1600 cm^{-1} is believed to arise from combinations and will be discussed later. Two of the three components of ν_4 are found at 701 cm^{-1} and 711 cm^{-1} while the third may either be the weaker band near 738 cm^{-1} or be unresolved from the 701 to 711 cm^{-1} doublet. The selection rules require ν_1 and ν_2 to be infrared active in species B_{1u} and B_{3u}. The two components of ν_1 can be assigned as the two sharp bands observed near 1050 cm^{-1} and 1072 cm^{-1} in the low temperature $SrCO_3$ spectra. There are undoubtedly a number of bands, partly unresolved, near the expected position for the two components of ν_2. Some of these are undoubtedly lattice combination modes but in any case there appears to be little difficulty in concluding that ν_2 consists of at least two components. Similar assignments are possible in the other aragonite type structures. It should be noted that Decius [14, 15] has pointed out that the out-of-plane bending modes in aragonite type crystals are strongly coupled as a result of the proximity of the anions. This coupling produces a splitting of ν_2 when isotopic species are involved. The relative intensities involved here, however, appear to be too great to be attributed to the natural abundance of isotopes.

Cubic structures. In the cubic structures the factor group selection rules show that the only active infrared species is F_u with six triply degenerate internal frequencies and eight triply degenerate lattice modes. The six internal frequencies are derived from ν_1 and ν_2 and two each from ν_3 and ν_4. ν_1 is observed very weakly if at all and can hardly be considered as an active fundamental. ν_2 can only be assigned near 812 cm^{-1}, its usual position. There may be two components of ν_3 but the great intensity of the band prevents any attempts to locate their positions. The splitting of ν_3 has been observed in the cubic structures by Couture and Mathieu [10] who studied the Raman spectrum. The two components of ν_4 must be considered unresolved in the band near 722 cm^{-1} in the cubic nitrates.

Some basis must be found for the assignment of the large number of nonfundamental frequencies some of which are very strong. These bands are observed in the low temperature spectra of all the nitrates and carbonates. The factor group treatment forms an adequate basis for assigning these bands as there are in principle no selection rules governing the combinations of lattice modes with internal modes [78]. However, there is no indication of the relative intensities to be expected for sum and difference bands.

3.3. Libration-Fundamental Summation and Difference Bands in the 700 cm^{-1} to 1500^{-1} Region

In this section the large number of bands occurring in the 700 cm^{-1} to 1500 cm^{-1} region of the spectrum are discussed. These bands will be interpreted tentatively as combinations between fundamental internal vibrations and a low-lying mode of the order of 20 cm^{-1}—30 cm^{-1}. The justification for considering the low frequency mode as a libration fundamental will be given later but the interpretation will be made in accordance with this hypothesis.

The proposed model is shown schematically in figure 2 which assumes an ion on a site of symmetry C_3. The potential energy curve for libration is represented by the broken curve on the ground state vibrational level ($n=0$) and the first excited vibrational level ($n=1$). The potential energy is assumed to be independent of the vibrational state. In each of the three potential wells there are seven excited librational levels ($J=1-J=7$) shown. These levels are shown evenly spaced, i.e., anharmonicity corrections are neglected. Transitions between energy states are indicated by the vertical lines. No transitions are indicated between librational levels in the same vibrational state because the energies involved are too low to be of interest here.

At any given temperature transitions in all three potential wells will be similar since the three configurations of the ion are equivalent. With this in mind the three potential minima of figure 2 are utilized to demonstrate the effect of temperature on the resulting spectrum. At very low temperatures where all ions are in the ground state, only summation bands are possible as indicated in the left potential minimum. At intermediate temperatures, in addition to the summation bands shown at the lowest temperature some difference bands arise from the thermal excitation of some ions into the lower librational levels in the ground vibrational level. At still higher temperatures, in addition to the previous transitions, lower energy difference bands arise from thermal excitation to the higher librational levels in the ground vibrational state. Transitions to rotational levels which exist above the potential barriers are not indicated in figure 2. All possible transitions are not shown except at the lowest temperature.

a. Calcite Type Structures

Many calcite type crystals show spectra which are lacking in detail although there is evidence of unresolved absorption in the region of interest. However, the spectra for $NaNO_3$ shown in figure 3 are most informative. It will be noted that the diffuse absorption between approximately 900 cm^{-1} and 1060 cm^{-1} at room temperature (top spectrum), is resolved at liquid helium temperature (lower spectrum) into a series of step like bands located at 913 cm^{-1}, 938 cm^{-1}, 963 cm^{-1}, 991 cm^{-1}, 1021 cm^{-1}, 1058 cm^{-1}, and 1071 cm^{-1}. These bands have a nearly uniform separation varying from about 25 cm^{-1} to 37 cm^{-1}. In the low temperature spectrum other bands are also resolved and the resulting observations are tabulated in table 4.

TABLE 4. *Assignments for* $NaNO_3$ *at liquid helium temperature for libration combinations*

Frequency	Separation from fundamental	Frequency	Separation from fundamental	Frequency	Separation from fundamental	Assignment
cm^{-1}	cm^{-1}	cm^{-1}	cm^{-1}	cm^{-1}	cm^{-1}	
727 (ν_4)		838 (ν_2)		1068 (ν_1)		ν_i
747 vw	20	?		1103 w	32	ν_i+L
776 vw	51	?		?		ν_i+2L
803 vw	75	913 m	75	1143 vw	75	ν_i+3L
?		938 m	100	1176 sh	108	ν_i+4L
?		963 m	125	1192 s	124	ν_i+5L
880 ?	153	991 s	153	1228 w	160	ν_i+6L
907 sh	180	1021 s	183	?		ν_i+7L
945 sh	218	1058 s	220	?		ν_i+8L
960 sh ?	233	1071 vs	233	1311 s	243	cutoff

Although they are diffuse and poorly defined at higher temperatures, the 913 cm^{-1} – 1071 cm^{-1} series of bands appear to shift by 3 cm^{-1} to 7 cm^{-1} between the temperature of liquid nitrogen and that of liquid helium with the larger shifts associated with the higher frequency bands. In the same temperature interval the fundamental ν_2 shows no detectable shift and ν_4 a shift of at most 1 cm^{-1}. From its temperature dependence and intensity it is believed that the 1071 cm^{-1} band represents the band limit or cutoff frequency of the series of bands starting at 913 cm^{-1} rather than the fundamental ν_1 which is inactive in all calcite structures. This series of bands may be interpreted as combinations of a mode of frequency 20 cm^{-1} – 30 cm^{-1} with ν_2. Similarly other bands in the structure may be interpreted as combinations of the same low frequency mode with ν_4 and the inactive ν_1 fundamental. The cutoff for the series of bands originating from ν_1 is believed to be the strong band at 1311 cm^{-1}. The cutoff for the series from ν_4 is not apparent but may tentatively be taken as a shoulder appearing at 960 cm^{-1}. The differences between the cutoff frequencies and the respective fundamentals for the three series of bands are 243 cm^{-1} (ν_1), 233 cm^{-1} (ν_2), and possibly 233 cm^{-1} (ν_4). The bands and assignments are given in table 4. These data as well as all other tabulated data refer only to observations at liquid helium temperature and include only libration-fundamental summation bands with ν_1, ν_2, and ν_4. Tabular data are recorded only for reproducible bands and where there is doubt about the existence of a band the recorded frequency is followed by a question mark. The following abbreviations are used in all tables: very weak—vw; weak—w; shoulder—sh; medium—m; strong—s; very strong—vs; broad—b. From the tabular data it will be noted that the correlation between the three series is reasonably good. The energy level spacing varies but the apparent variation is estimated to be of the same order of magnitude as the error associated with determining the positions of the weak, frequently broad, combination bands.

Although no combination bands of the 20 cm^{-1}—30 cm^{-1} mode with ν_3 are tabulated for any spec-

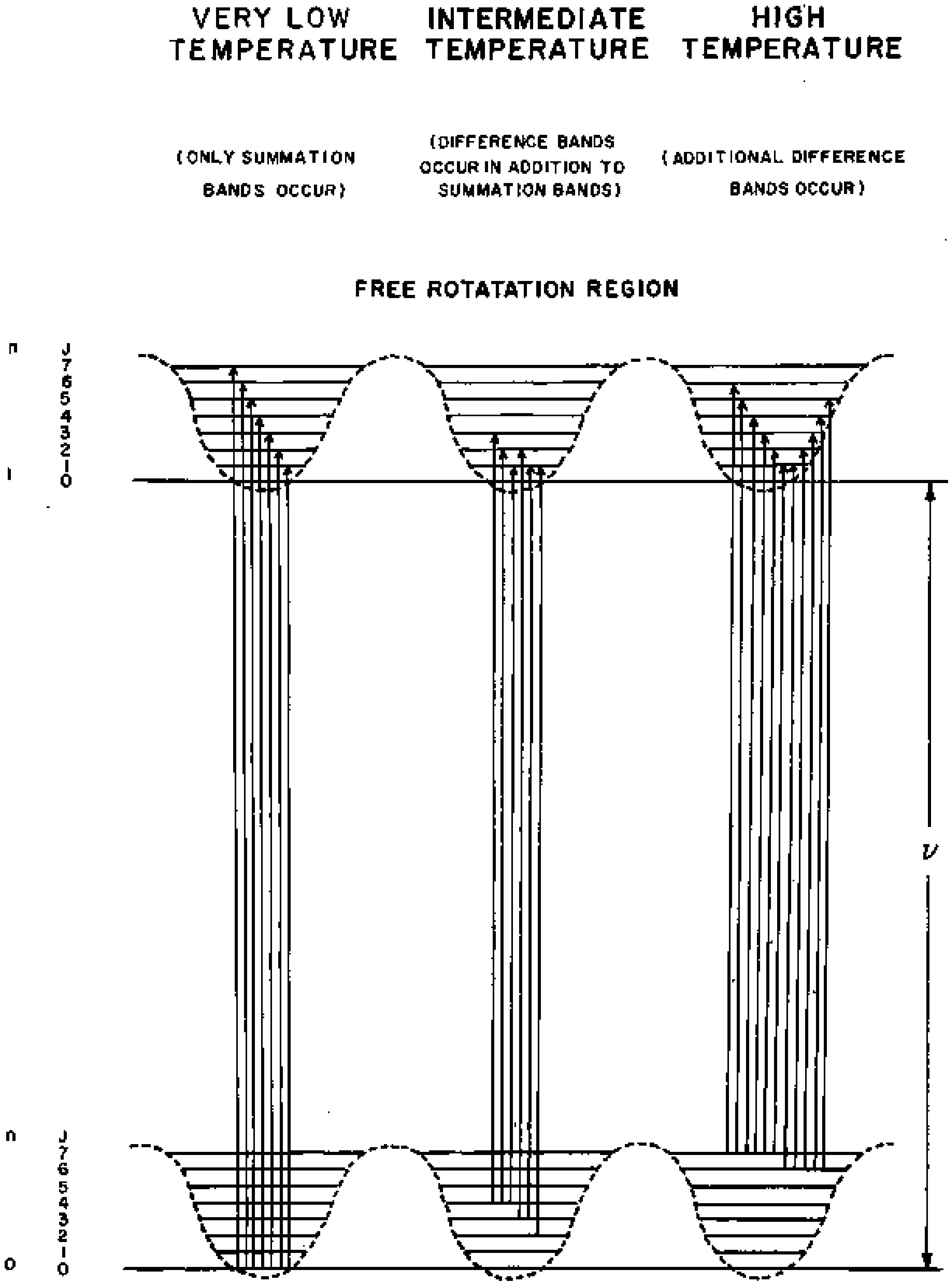

Figure 2. *Energy level diagram for effect of temperature on libration-vibration combination bands.*

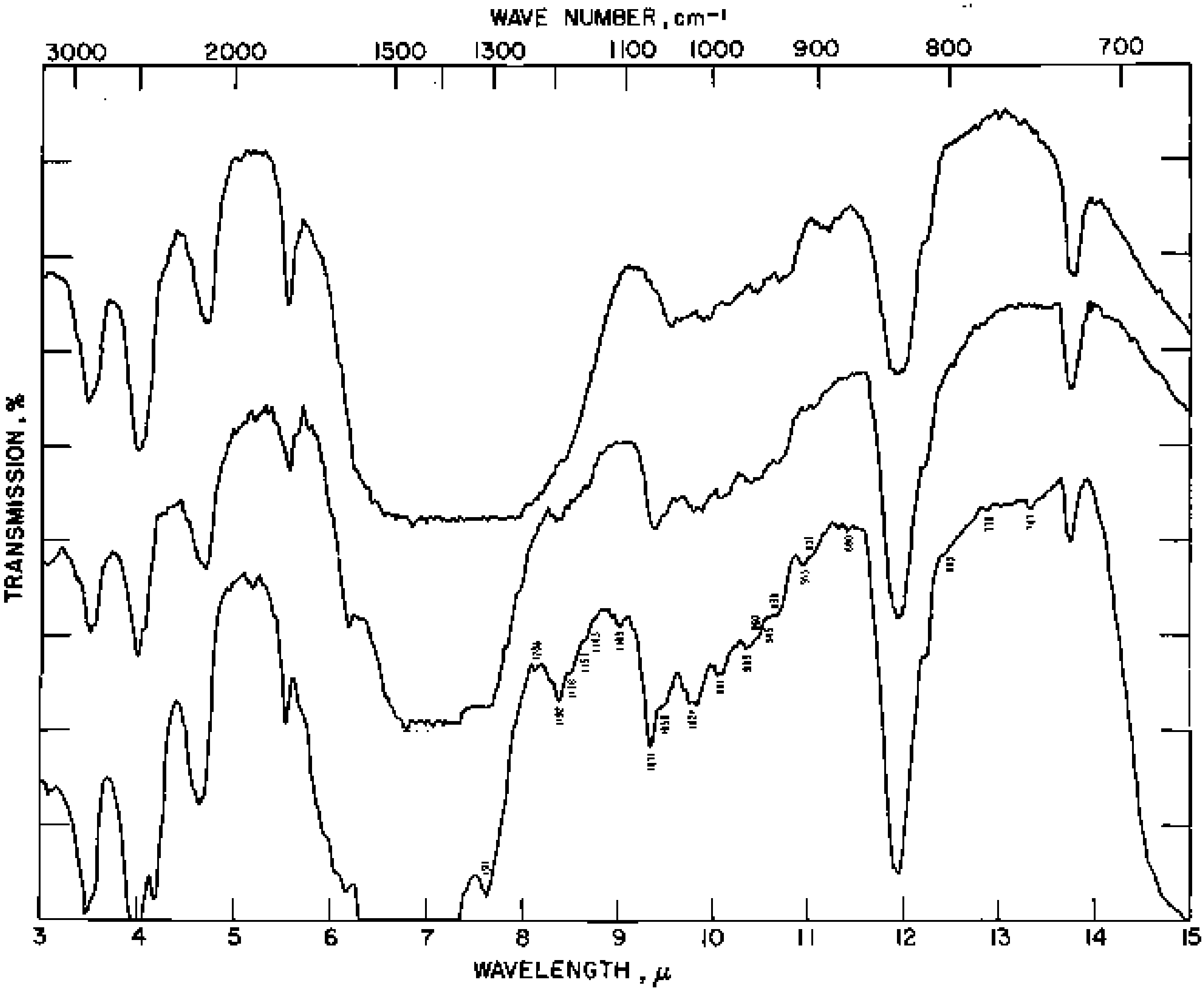

Figure 3. *Infrared absorption spectra of* $NaNO_3$ *at room temperature (top), liquid nitrogen temperature (center), and liquid helium temperature (bottom).*

trum many instances of summation bands originating from ν_3 have been observed. In this frequency region the instrumental dispersion is too low and the intensity of ν_3 is usually too great to permit location of combinations with any certainty. Evidence for the existence of combinations with ν_3 is indicated by figure 3 and all subsequent figures. The marked increase in transmission of all crystals on the low frequency side of ν_3 as the temperature is lowered may be attributed to the elimination of difference bands between ν_3 and a low frequency mode at lower temperatures. A corresponding change does not occur on the high frequency side of ν_3, where the summation bands would be expected to become stronger at lower temperatures. Furthermore, the rather abrupt increase in transmission observed in most spectra on the high frequency side of ν_3 occurs at a frequency which is of the correct order of magnitude for the cutoff for a series of combination bands originating from the fundamental ν_3.

Although the assignments given in table 4 account for all bands it cannot be considered completely satisfactory. Several expected bands are missing and the band at 1192 cm^{-1} is unexpectedly strong. A similar situation will be encountered in all other spectra. All assignments, therefore, are made with some qualifications.

Spectra at room temperature and liquid helium temperature are given for the other calcite structures $MgCO_3$, $CaCO_3$, $FeCO_3$, and $MnCO_3$ in figures 4, 5, 6, and 7 respectively with tabular data for $CaCO_3$ listed in table 5. Satisfactory resolution of bands was not obtained on any specimen of $MgCO_3$ despite several experiments on crystals of differing thicknesses. The strong band near 1250 cm^{-1} may represent the ν_1 cutoff and that near 1120 cm^{-1} the ν_2 cutoff. A low frequency mode of about 25 cm^{-1} and a cutoff frequency of approximately 230 cm^{-1} are indicated on the basis of the several experiments.

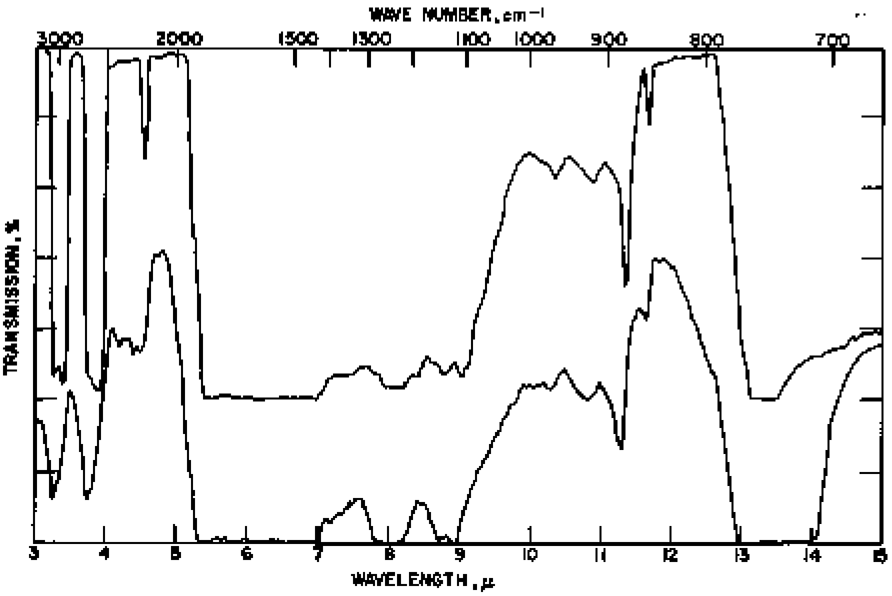

FIGURE 4. *Infrared absorption spectra of* $MgCO_3$ *at room temperature (top) and liquid helium temperature (bottom).*

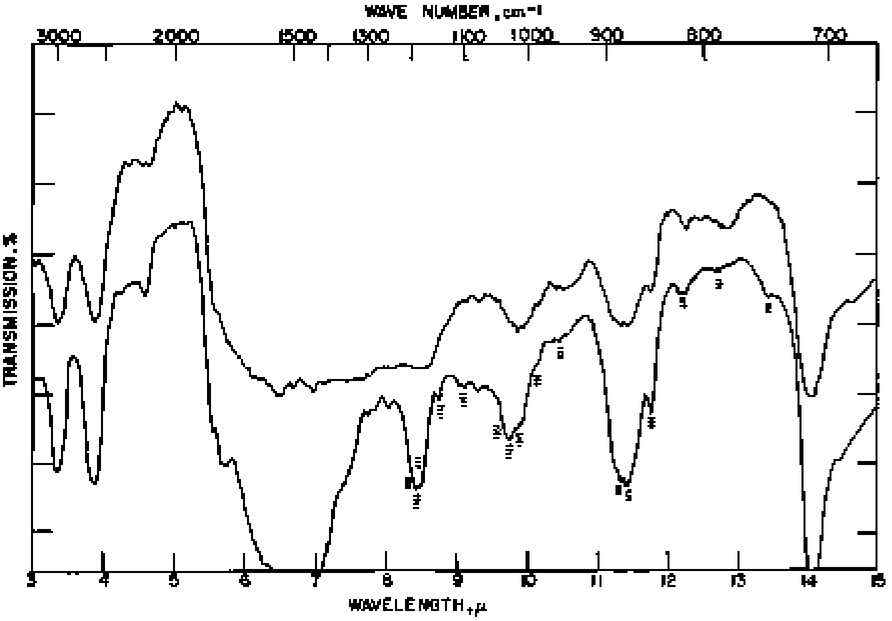

FIGURE 5. *Infrared absorption spectra of* $CaCO_3$ *(calcite) at room temperature (top) and liquid helium temperature (bottom).*

TABLE 5. *Assignments for* $CaCO_3$ *at liquid helium temperature for libration combinations*

Frequency	Separation from fundamental	Frequency	Separation from fundamental	Frequency	Separation from fundamental	Assignment
cm⁻¹	*cm⁻¹*	*cm⁻¹*	*cm⁻¹*	*cm⁻¹*	*cm⁻¹*	
712 (ν_4)		881 (ν_2)		1070 (ν_1)		ν_4
746 m	34	?	?	1103 w	33	ν_4+L
784 w	72	953 w	72	1142 m	72	ν_4+2L
819 m	107	990 sh	109	1177 s	107	ν_4+3L
850? s	138	1015 s	134	1190 s	116	ν_4+4L
Cutoff masked by ν_2	?	1028 s	147	1199 sh	133	ν_4+5L
		1034?	153	1220	150	cutoff

Tabular data for $CaCO_3$ are given in table 5. A libration frequency of about 35 cm^{-1} and an average cutoff frequency of about 150 cm^{-1} are indicated. Three weak bands at 1075 cm^{-1}, 1245 cm^{-1}, and 1283 cm^{-1} are not accounted for by the assignments. Although the band at 1075 cm^{-1} might be taken as the inactive ν_1 fundamental this is not believed to be the case. Raman spectroscopy has located ν_1 near 1086 cm^{-1} and this fundamental is invariably observed as a sharp band in the infrared spectrum when it is active. The band at 1075 cm^{-1} however, is quite broad.

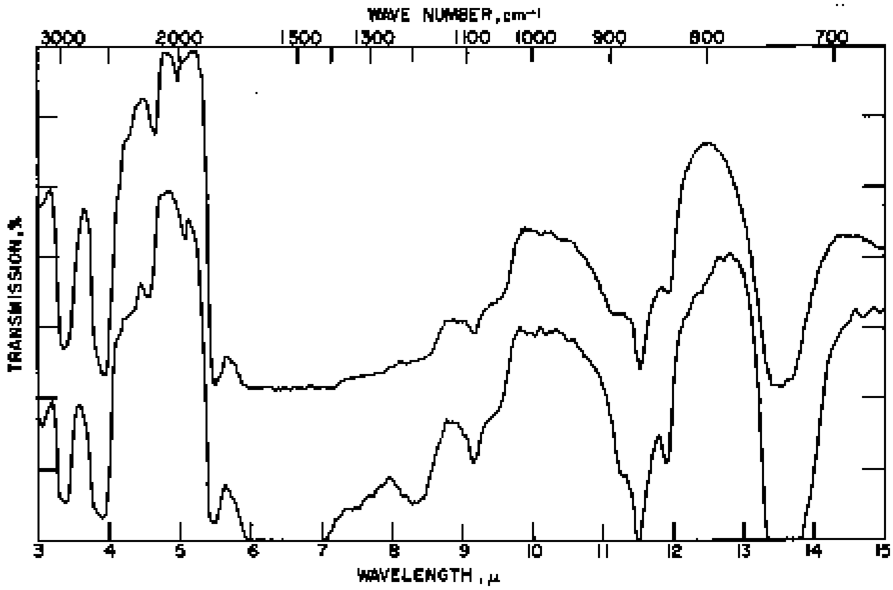

Figure 6. *Infrared absorption spectra of* $FeCO_3$ *at room temperature (top) and liquid helium temperature (bottom).*

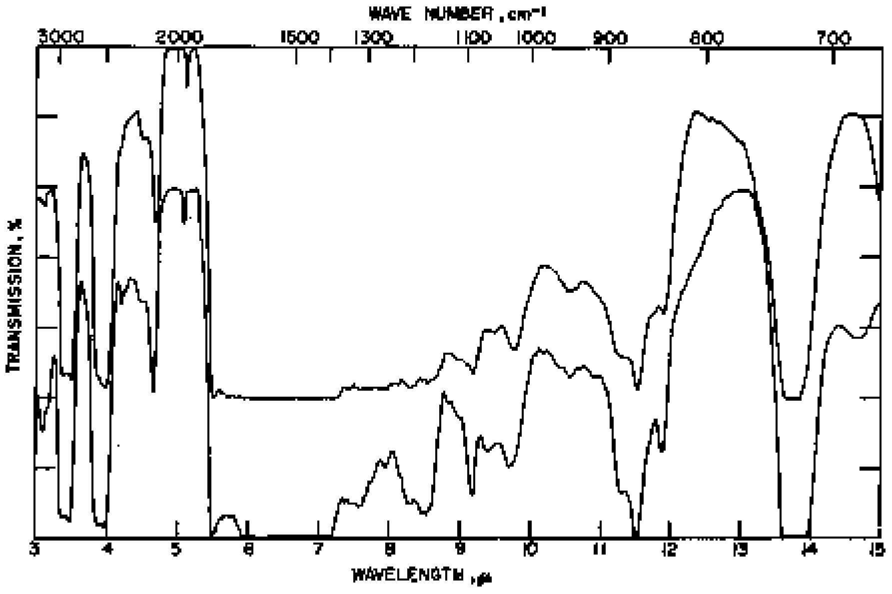

Figure 7. *Infrared absorption spectra of* $MnCO_3$ *at room temperature (top) and liquid helium temperature (bottom).*

No data are tabulated for $FeCO_3$ and $MnCO_3$ because of the questionable purity of the specimens. As shown by the spectra both materials exhibit the same general absorption pattern as the other calcite structures. Cutoff frequencies are estimated to be 150 cm^{-1} for $FeCO_3$ and 160 cm^{-1} for $MnCO_3$ on the basis of tentative assignments. The $MnCO_3$ spectrum which shows much fine structure can be interpreted with a single libration frequency of 15 cm^{-1} or with two separate frequencies of 30 cm^{-1}.

b. Aragonite Type Structures

Spectra for two temperatures are given for $SrCO_3$ in figure 8 and the tabular frequencies observed in table 6. Spectra at room temperature and liquid He temperature and the tabulated frequencies are given in figures 9, 10, 11, and 12, and tables 7, 8, 9, and 10 for $CaCO_3$ (aragonite), $BaCO_3$, $PbCO_3$, and KNO_3 respectively. Additional expanded spectra at liquid helium temperatures covering the range from about 1800 cm^{-1} to 770 cm^{-1} for $SrCO_3$ and $CaCO_3$ (aragonite) are given in figures 13 and 14.

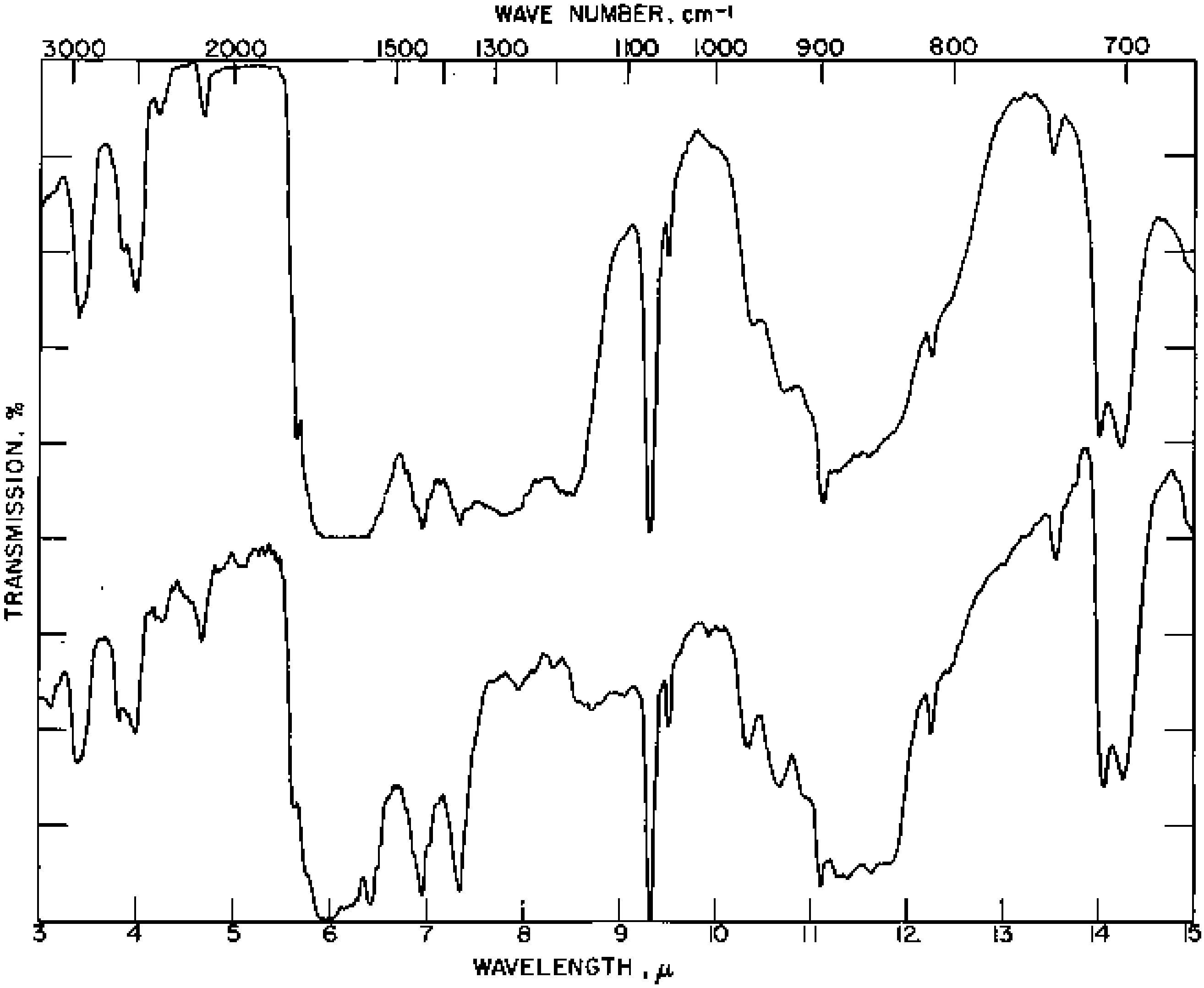

FIGURE 8. *Infrared absorption spectra of $SrCO_3$ at room temperature (top) and liquid helium temperature (bottom).*

TABLE 6. *Observed frequencies for $SrCO_3$ at liquid helium temperature*

Frequency	Separation from fundamental	Frequency	Separation from fundamental	Frequency	Separation from fundamental
cm⁻¹	cm⁻¹	cm⁻¹	cm⁻¹	cm⁻¹	cm⁻¹
701 711 } ν_4		863 ν_2		1072 ν_1	
				1108 vw	36
737 ν_4?	30?	908 vw	45	1147 vb	75
803 wb	92?	919 mb	60	1165 vb	93
816 s	105?	937 mb	73	1200 w	128
861 sb	150?	967 sb	104	1230 w	158
879 sb	168?	995 vw	132	1256? w	184
900 s	189?	1009 vw	146	1261? w	189
		1042 w sh	179		
		1050 m	187		

TABLE 7. *Observed frequencies for $CaCO_3$ (aragonite) at liquid helium temperature*

Frequency	Separation from fundamental	Frequency	Separation from fundamental	Frequency	Separation from fundamental
cm⁻¹	cm⁻¹	cm⁻¹	cm⁻¹	cm⁻¹	cm⁻¹
701 717 } ν_4		866 ν_2		1086 ν_1	
—		—		1102 s	16
741 mb	24?	—		1110 sh	24
—		—		1121 m	35
—		—		1133 msh	47
775 w	58?	924 w	58	1144 s	58
—		—		1148 sh	62
—		—		1155 wsh	69
809? sh	92?	—		1176 sh	90
—		969 w	103	1182 w	96
—		983 w	117	1201 m	115
839 sb	122?	989 w	123	—	
846? sb	129?	996 sh	130	1215 m	129
—		1008 w sh	142	—	
—		—		1245 w	159
883 sb	166?	1034 b	168	1254 w	168
903 b	184?	1055 wb	189	1278 sh	192
912 s	195?	1061 m	195	1291 mb	205

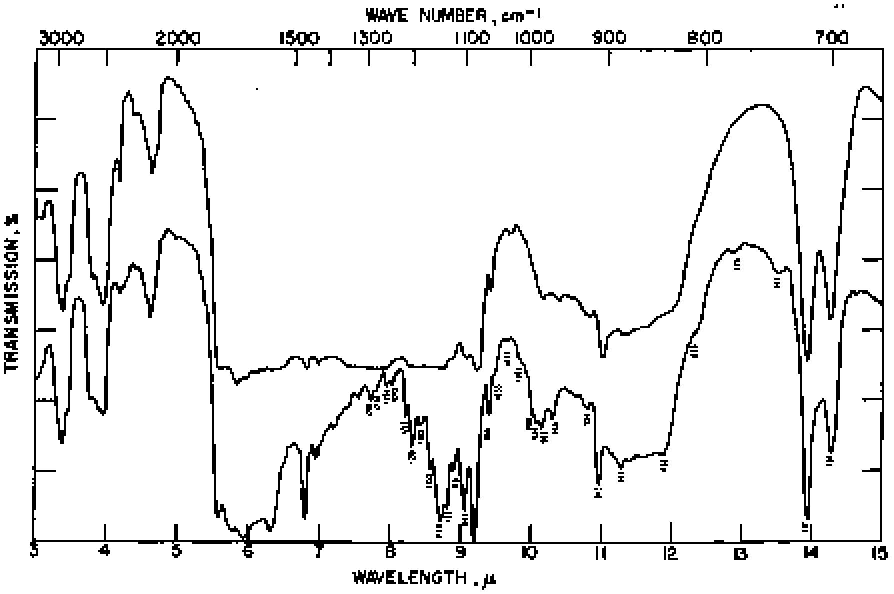

FIGURE 9. *Infrared absorption spectra of* $CaCO_3$ *(aragonite) at room temperature (top) and liquid helium temperature (bottom).*

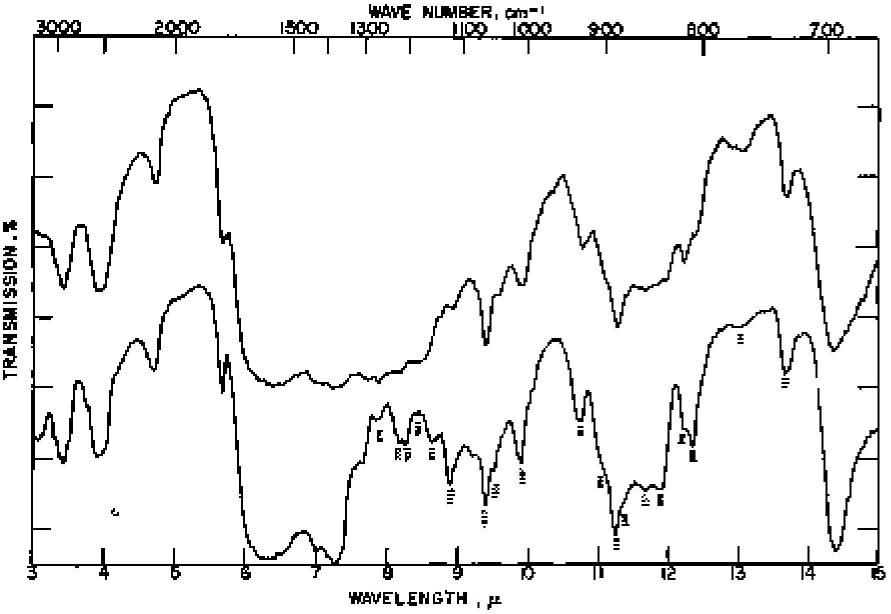

FIGURE 10. *Infrared absorption spectra of* $BaCO_3$ *at room temperature (top) and liquid helium temperature (bottom).*

TABLE 8. *Observed frequencies for* $BaCO_3$ *at liquid helium temperature*

Frequency	Separation from fundamental	Frequency	Separation from fundamental	Frequency	Separation from fundamental
cm^{-1}	cm^{-1}	cm^{-1}	cm^{-1}	cm^{-1}	cm^{-1}
694 ν_4		857 ν_2		1062 ν_1	
732 m (ν_4?)	38	900 m	43	1075 ?	13
770 vw	76	932 m	75	1123 m	61
808 m	114	—		1154 m	92
818 sh	124	—		1184 vw	122
840 s	156	1007 m	150	1212 m	150
880 sh	186	1038 w sh	181	1222 m	160
888 s	194	1051	194	—	

TABLE 9. *Observed frequencies for* $PbCO_3$ *at liquid helium temperature*

Frequency	Separation from fundamental	Frequency	Separation from fundamental	Frequency	Separation from fundamental
cm^{-1}	cm^{-1}	cm^{-1}	cm^{-1}	cm^{-1}	cm^{-1}
684 ν_4		842 ν_2		1057 ν_1	
727 m ν_4?	42	896 w sh	54	1082 w	25
734 m ν_4?	50	911 w	69	1101 sh	43
—		—		1118 s	61
768 vw	84	925 w sh	83	1143 sh	86
788 mb	104	938 w sh	96	1161 w	104
797 mb	113	958 w sh	116	—	
809 wb	125	977 w sh	135	1187 w	130
818 vw	134	—		—	
827 m	143	996 vw	154	—	
854 sb	170	1011 vw	169	1228 m	171
—		1022 wb	180	1234 m	177
877 s	193	1036?	194	1257 m sb	200 cutoff?

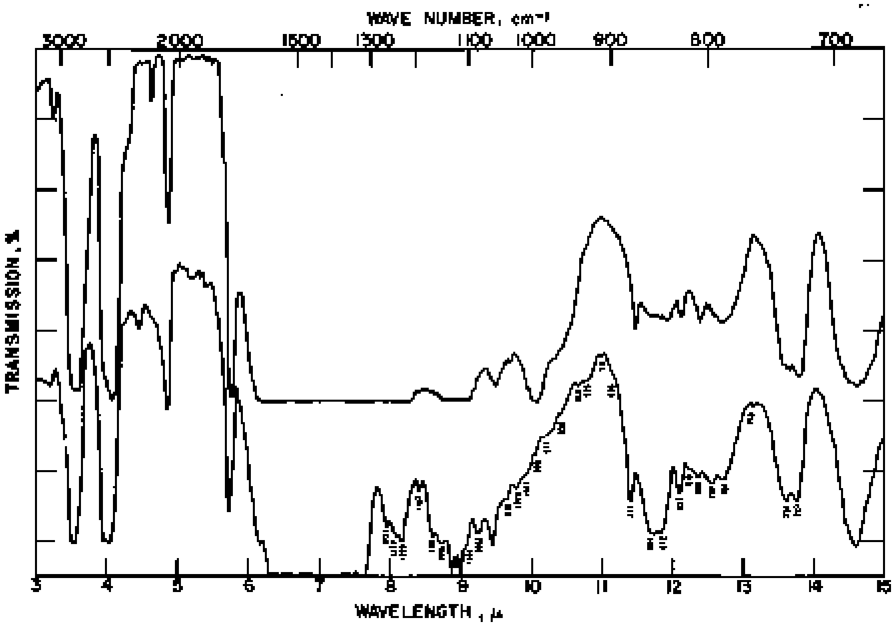

FIGURE 11. *Infrared absorption spectra of* $PbCO_3$ *at room temperature (top) and liquid helium temperature (bottom).*

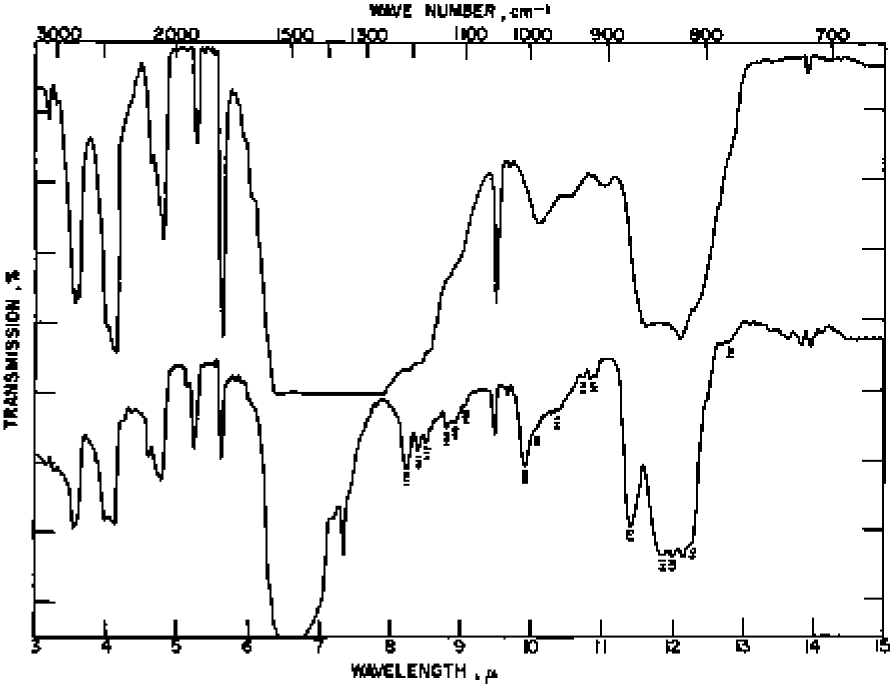

FIGURE 12. *Infrared absorption spectra of* KNO_3 *at room temperature (top) and liquid helium temperature (bottom).*

Only general observations are given for these spectra. Attempts to analyze the highly complex structure observed in figures 13 and 14 have met with only indifferent success. In part, this is probably the result of the more complex internal fundamental bands observed in these structures which were discussed earlier. At the very least this would produce many overlapping band systems. In part the complexity may arise from further splitting of ν_3 from isotope effects first noted by Decius [15] in the aragonites. Finally, there are strong indications that at least two libration frequencies may be involved in these spectra to produce still greater overlapping.

That combination modes are involved is clearly shown by comparing the normal and low temperature spectra. Elimination of the difference modes with ν_1 is clearly seen in figures 9, 10, and 11 so that there is little doubt that a liberation frequency of approximately 30 cm^{-1} is present. Attempts have been

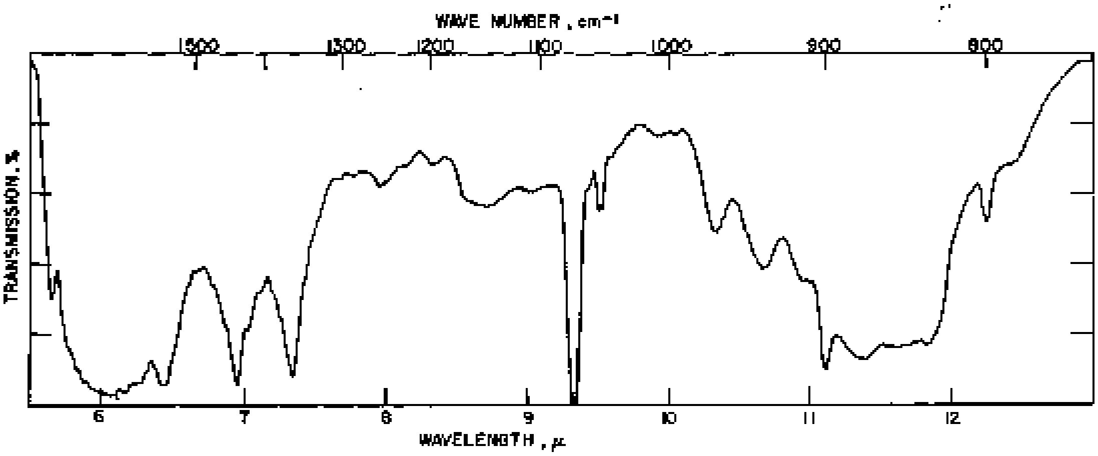

Figure 13. *Infrared absorption spectrum of* $SrCO_3$ *at liquid helium temperature (expanded scale).*

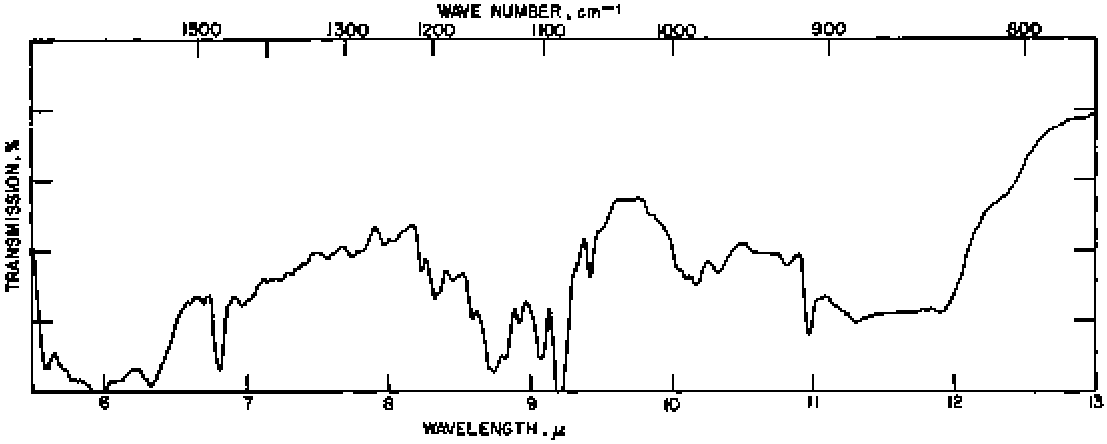

Figure 14. *Infrared absorption spectrum of* $CaCO_3$ *(aragonite) at liquid helium temperature (expanded scale).*

Table 10. *Observed frequencies for* KNO_3 *at liquid helium temperature*

Frequency	Separation from fundamental	Frequency	Separation from fundamental	Frequency	Separation from fundamental
cm^{-1}	cm^{-1}	cm^{-1}	cm^{-1}	cm^{-1}	cm^{-1}
714 ν_4		827 ν_2		1051 ν_1	
—		—		1100 wb	49
782	68	—		1119 b	68
—		921? b	94	1133 mb	82
815 s	101	930 vw	103	—	
833 b	119	—		1172 m	121
843 b	129	960 wb	139	1187 m	136
875 s	161	991 w sb	164	1213 s	162
		1008 s	181		

made to correlate bands arising from the various fundamentals in the tabular data. It appears that correlations exist despite the failure to analyze the data.

One outstanding characteristic of the carbonate aragonites is to be found in the very broad, intense band found in the ν_2 region. This band completely obscures the ordinarily strong ν_2 band found in thin polycrystalline films of these materials [77]. The sharp strong band on the high frequency edge of this absorption complex does not correspond to the usual out-of-plane bending frequency, but may represent the cutoff for a series of liberation modes with ν_4.

c. Cubic Type Structures

The spectra of the cubic nitrates show many bands falling into a regular series that may be assigned to combinations between a harmonic liberation mode and the fundamentals ν_1, ν_2, and ν_4. Spectra at three temperatures are shown for $Pb(NO_3)_2$ in figure 15 while similar spectra at two temperatures are given in figures 16 and 17 for $Ba(NO_3)_2$ and $Sr(NO_3)_2$ respectively. Assignments at liquid helium temperature are tabulated in tables 11, 12, and 13. In the spectra it is noted that bands falling between 850 cm^{-1} and 1250^{-1} have relatively large frequency shifts with temperature, while the fundamentals ν_2 and ν_4 appear to be unaffected by the same temperature change. These bands may be attributed to the combinations of a low lying librational mode with the fundamentals, with the librational mode being relatively temperature dependent through the effect of expansivity on volume.

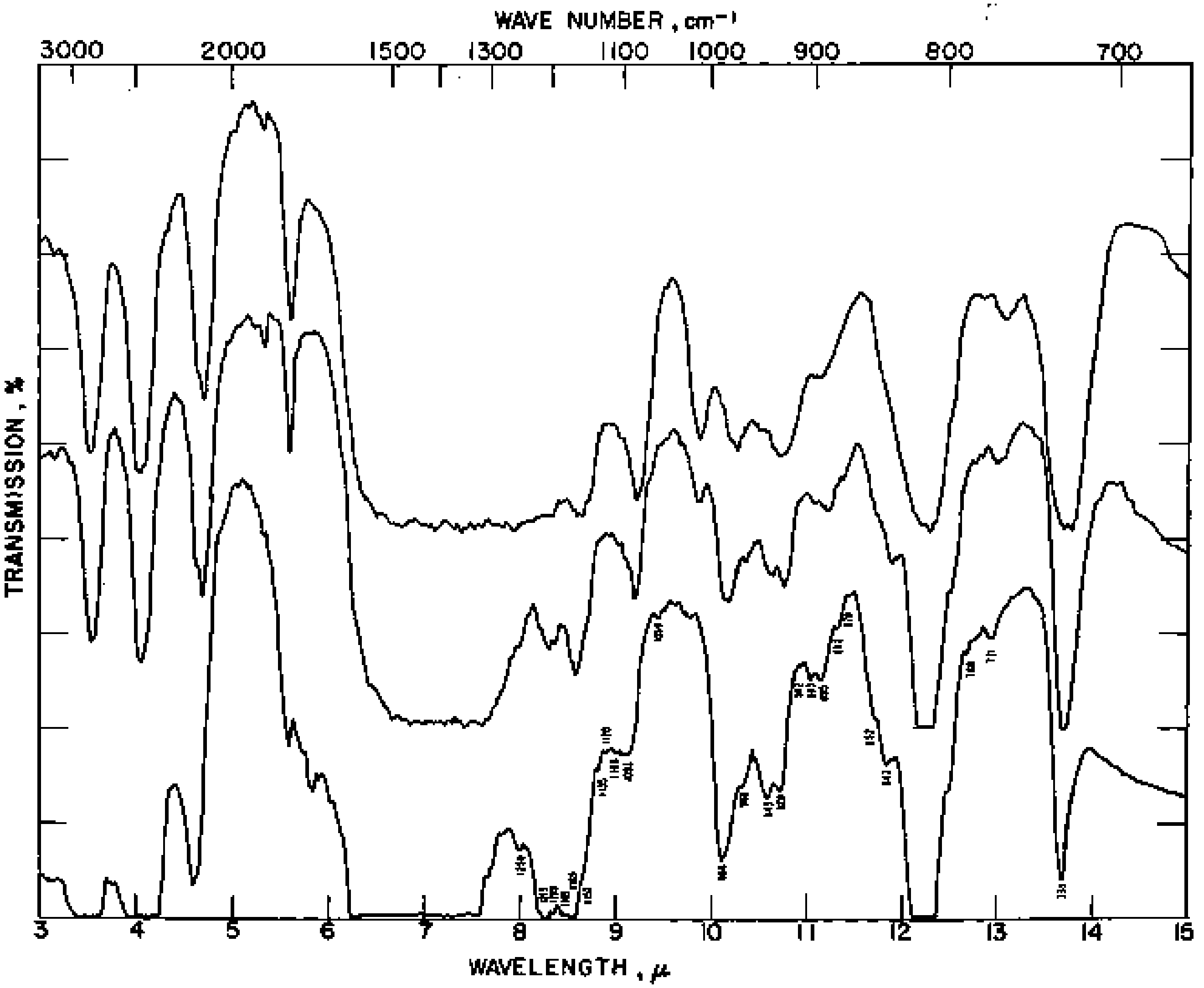

FIGURE 15. *Infrared absorption spectra of* $Pb(NO_3)_2$ *at room temperature (top), liquid nitrogen temperature (center), and liquid helium temperature (bottom).*

TABLE 11. *Assignments for* $Pb(NO_3)_2$ *at liquid helium temperature for libration combinations*

Frequency	Separation from fundamental	Frequency	Separation from fundamental	Frequency	Separation from fundamental	Assignment
cm⁻¹	cm⁻¹	cm⁻¹	cm⁻¹	cm⁻¹	cm⁻¹	
731 ν_4		817 ν_2		1058 ν_1		ν
—		838 ?	21	—		$\nu+L$
771	40	852 sh	35	1093 s	35	$\nu+2L$
788	57	—		ν_3 1109 vw	51	$\nu+3L$
?		883 m	66	1120? vw	62	$\nu+4L$
?		—		1136 sh	77	$\nu+5L$
?		912 vw	95	1152 sh	94	$\nu+6L$
843	113	928 s	111	1169 s	111	$\nu+7L$
858 sh	127	943 s	126	1183 sh	125	$\nu+8L$
878 sh	147	963 s	146	1199 sh	141	$\nu+9L$
895	164	—		1212 vs	163	$\nu+10L$
903	172	988 vs	171	1220	182	cutoff

TABLE 12. *Assignments for* $Ba(NO_3)_2$ *at liquid helium temperature for libration combinations*

Frequency	Separation from fundamental	Frequency	Separation from fundamental	Frequency	Separation from fundamental	Assignment
cm⁻¹	cm⁻¹	cm⁻¹	cm⁻¹	cm⁻¹	cm⁻¹	
722 ν_4		813 ν_2		1052 ν_1		ν
—		—		—		$\nu+L$
765	43	—		1086 vs	34	$\nu+2L$
785 b	63	866 vw	53	1105 m sh	53	$\nu+3L$
—		—		1125 s	73	$\nu+4L$
—		—		1139 s	87	$\nu+5L$
—		—		1156 s	104	$\nu+6L$
838 sh	116	931 m	118	1172 w sh	120	$\nu+7L$
857 w	136	949 m	136	1188 sh	136	$\nu+8L$
876 w	154	969 m	156	1209 sh	157	$\nu+9L$
889 sh	167	982 sh	169	1220 ?	168	$\nu+10L$
898 s	176	993 s	180	1231 s	179	$\nu+11L$
?		?		?		$\nu+12L$
913 m	191	1004	191	1245	193	cutoff

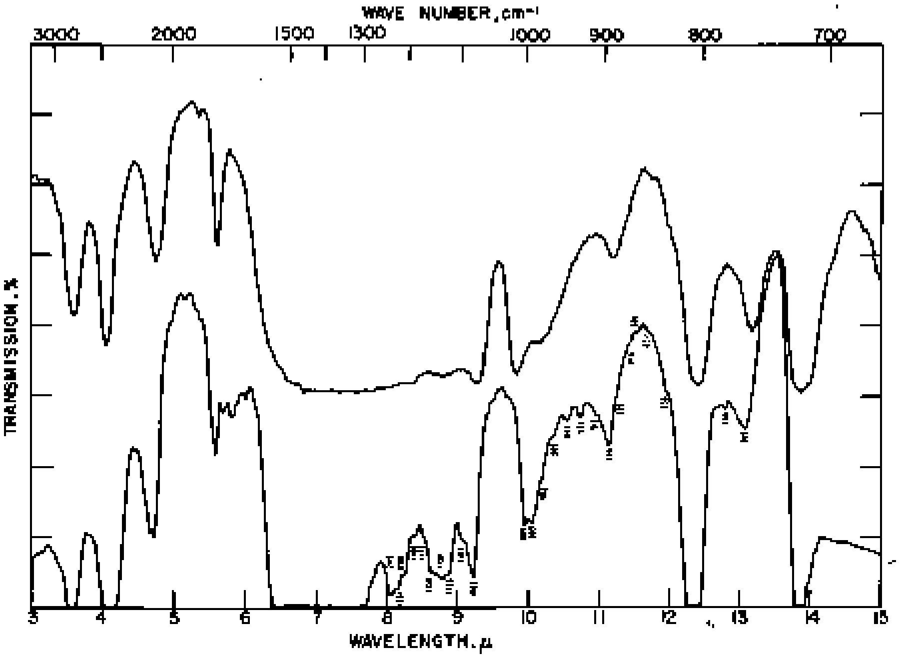

FIGURE 16. *Infrared absorption spectra of* $Ba(NO_3)_2$ *at room temperature (top) and liquid helium temperature (bottom).*

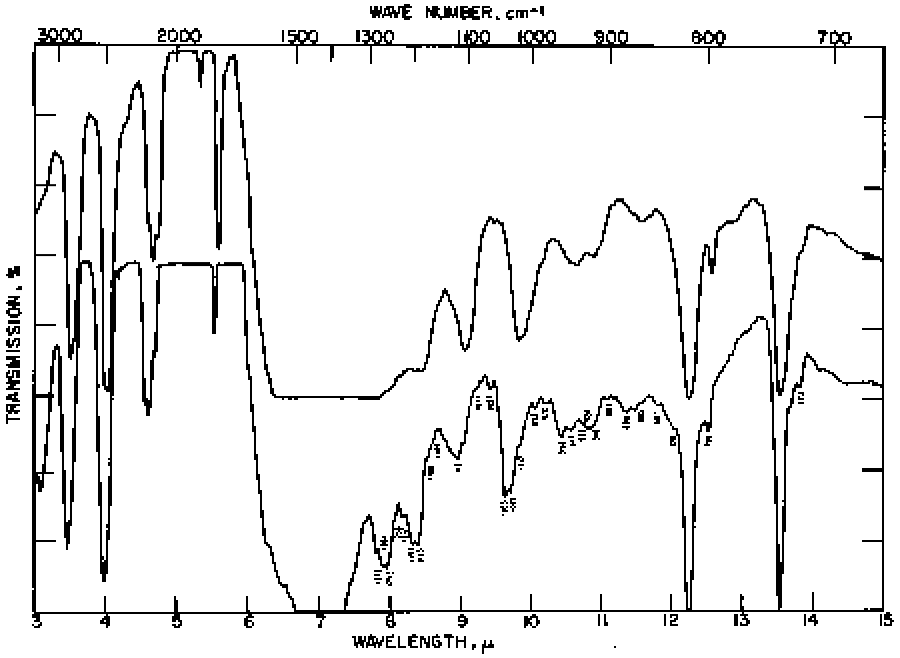

FIGURE 17. *Infrared absorption spectra of* $Sr(NO_3)_2$ *at room temperature (top) and liquid helium temperature (bottom).*

Inspection of the tables shows a rather systematic series of bands arising from each of the fundamentals. In the region between ν_2 and the cutoff for the series arising from ν_4 the band structure is highly complex. Assignments in this region are not unequivocal as may be seen from the vacancies in the tables. The combination bands are neither sharp nor strong so that errors in positions may easily amount to a few cm^{-1}. With this uncertainty the variation in spacing appears to be of the order of the errors in locating the bands.

The behavior of the two bands located symmetrically on either side of the inactive or very weak ν_1 frequency (circa 1050 cm^{-1}) provide a convincing argument for the assignments given. These bands are believed to arise from sum and difference tones of the libration and the symmetric stretch. In the room temperature spectra these bands are very

TABLE 13. *Assignments for* $Sr(NO_3)_2$ *at liquid helium temperature for libration combinations*

Frequency	Separation from fundamental	Frequency	Separation from fundamental	Frequency	Separation from fundamental	Assignment
cm^{-1}	cm^{-1}	cm^{-1}	cm^{-1}	cm^{-1}	cm^{-1}	
739 (ν_4)		815 ν_2		1057 ν_1		ν_0
754 ?	16	829 sh	14	1077 sh	20	ν_0+L
...		?		—		ν_0+2L
799 s	60	?		1112 s b	55	ν_0+3L
—		?		—		ν_0+4L
830 sh	91	?		1149 vw	92	ν_0+5L
847 w	109	924 m	109	1168 w sh	111	ν_0+6L
865 w	127	?		1185 s	128	ν_0+7L
880 m	142	?		1197 s	140	ν_0+8L
900 ? vw	162	976 w	161	1217 m	160	ν_0+9L
916 w sh	178	993 m	178	1236 sh	179	ν_0+10L
932 sh	194	1012 sh	197	1252 s	195	ν_0+11L
947 m	209	1027 sh	212	1264 s	208	ν_0+12L
959 s	220	1035 vs	220	1278 m	221	cutoff

prominent features of the spectra. In Sr $(NO_3)_2$ the bands appear to be located at 1103 cm^{-1} and 1029 cm^{-1} and the difference between these values appears to be four times the librational frequency giving a libration mode of 19 cm^{-1}. In $Pb(NO_3)_2$ the bands are at 1086 cm^{-1} and 1012 cm^{-1} giving $L = 18$ cm^{-1}, while in $Ba(NO_3)_2$ the corresponding values are 1074 cm^{-1}, 1015 cm^{-1} with $L = 15$ cm^{-1}. These values of the librational frequency may be lower than the corresponding values given in the tables for liquid helium temperature, but the value of the libration frequency is temperature dependent as shown by the temperature dependence of the libration bands. From figure 15 it will be noted that as the temperature is lowered the summation band located at 1086 cm^{-1} at room temperature in $Pb(NO_3)_2$ shifts to about 1088 cm^{-1} at liquid nitrogen temperature and to approximately 1093 cm^{-1} at liquid helium temperature. Simultaneously the difference band located at 1012 cm^{-1} which is very strong at room temperature is reduced to about one-half of this intensity at liquid nitrogen temperature and to a very weak, questionable band at liquid helium temperature. The intensity behavior corroborates the interpretation as a difference band and the low temperature required for its removal is conclusive evidence for a low frequency transition. As mentioned earlier this difference band constitutes a thermometer in the spectrum.

The effect of temperature on the cutoff frequency for combinations with ν_2 observed in the same figure appears to result in an increase of the cutoff from 975 cm^{-1} at room temperature, to 985 cm^{-1} at liquid nitrogen temperature and to about 988 cm^{-1} at liquid helium temperature. Simultaneously the cutoff appears to increase in intensity and become noticeably sharper. The effect of temperature on the intensity will be discussed later.

An analagous behavior is exhibited by $Sr(NO_3)_2$ and $Ba(NO_3)_2$. It should be noted that the strong 1015 cm^{-1} band in the room temperature spectrum of $Ba(NO_3)_2$ does not represent the cutoff for the ν_2 series. The 1015 cm^{-1} band is the ν_1 difference mode and is eliminated on cooling. The ν_2 series cutoff appears to be represented by the strong shoulder near 980 cm^{-1} which shifts to 1004 cm^{-1} on cooling. In $Sr(NO_3)_2$ the difference band located near 1015 cm^{-1} at room temperature appears to be obliterated by the ν_2 cutoff which shifts from an unknown position at room temperature to about 1032 cm^{-1} at liquid nitrogen temperature and to approximately 1035 cm^{-1} at liquid helium temperature.

As in all other spectra the effect of cooling on ν_3 is to produce a marked increase in transmission on the low frequency side of ν_3 with an absence of a similar effect on the high frequency side. This is in accord with the elimination of the difference modes ν_3-nL on cooling with no corresponding elimination of the summation bands. The ν_3 cutoff is estimated to be of the correct order of magnitude if it is taken at the frequency at which the specimens show transmission on the high frequency side of ν_3.

d. Miscellaneous Structure Types

Data are given here for $TlNO_3$, $AgNO_3$, $CsNO_3$, and $RbNO_3$. Spectra are given at three temperatures for $TlNO_3$ in figure 18. Spectra for two temperatures are given in figures 19, 20, and 21 for $AgNO_3$, $CsNO_3$, and $RbNO_3$, respectively. The corresponding frequencies are given in tables 14, 15, 16, and 17. In the experiments using $AgNO_3$ difficulties were encountered because of the reaction between the copper bar and $AgNO_3$. Successful runs were obtained by cementing the $AgNO_3$ crystal to a silver strip which was attached to the copper bar. The thermal path for $AgNO_3$ was longer and more doubtful than for any other specimen. However, comparison of the two spectra for the $AgNO_3$ show that considerable cooling was effected.

These spectra contain a wealth of fine structure of which only a portion appears to be explained by the present analysis. There are indications that at least two low frequency libration modes are coupling with the fundamentals giving rise to two overlapping series of bands with two cutoff values. As shown in table 14, half of the bands for $TlNO_3$ can be assigned with a 25 cm^{-1} libration mode but there are also at least nine unassigned bands.

TABLE 14. *Assignments for* $TlNO_3$ *at liquid helium temperature for libration combinations*

Frequency	Separation from fundamental	Frequency	Separation from fundamental	Frequency	Separation from fundamental	Assignment
cm^{-1}	cm^{-1}	cm^{-1}	cm^{-1}	cm^{-1}	cm^{-1}	
715 ν_4		828 ν_2		1044 ν_1		ν_0
740 s	25	860 sh	32	1068 sh	24	ν_0+L
—		—		1090 m	46	?
768 sh	53	880 sh	53	1096 m	52	ν_0+2L
		—		1101 sh	57	?
791 m	76	906 w	77	1115 w	71	ν_0+3L
—		913 sh	85	1127 vw	83	?
—		—		1138 w	94	?
—		931 w	103	1147 s	103	ν_0+4L
—		—		1150 vs	106	?
—		—		1160 sh	116	?
—		—		1168 sh	124	?
—		956 m	128	1175 s	131	ν_0+5L
860 sh	145	975 s	147	1193 b sh	149	?
865 w	160	989 m	161	1207 m	163	?
—		1003 s	175	1224 m	180	ν_0+7L
—		1023 m	195	—		?
922 w	207	1030	202	1246 w	202	ν_0+8L
943 sh	228	1054 vw	226	1290? sh	246	ν_0+9L
975 s	260	1080 m	252	1294? b	250	cutoff

TABLE 15. *Observed frequencies in $AgNO_3$ at liquid helium temperature*

Frequency	Separation from fundamental	Frequency	Separation from fundamental	Frequency	Separation from fundamental
cm^{-1}	cm^{-1}	cm^{-1}	cm^{-1}	cm^{-1}	cm^{-1}
—		806 ν_1		1046 ν_1	
711 ν_4		835	29	1078 s	32
735 ν_4		—		1086	40
—		—		1093	47
—		862 sh	56	1103 s	57
—		868	62	—	
—		—		1122 m	76
—		897	91	1136 m	90
—		909	103	1160 m	104
—		929	123	1164 sh	118
—		—		1179 sh	133
—		949	143	1195 m	149
—		—		1214 w	168
—		967	161	1230 sh	184
—		1000	195	1242 s	196
—		1017	211	—	
960	225	1025	219	Obscured?	cutoff?

TABLE 16. *Assignments for $CsNO_3$ at liquid helium temperature for libration combinations*

Frequency	Separation from fundamental	Frequency	Separation from fundamental	Frequency	Separation from fundamental	Assignment
cm^{-1}	cm^{-1}	cm^{-1}	cm^{-1}	cm^{-1}	cm^{-1}	
719 ν_4		833 ν_2		1058 ν_1		ν_0
—		860	27	—		ν_0+L
764 mb	45	880 wb	47	1108 s	50	ν_0+2L
797 vw	78	900 w	67	1129 s	71	ν_0+3L
?		933 m	100	1152 m	99	ν_0+4L
?		956 s sh	123	1178 sh	125	ν_0+5L
?		980 vs	147	1185 s	132	?
≈880 b	163	994 vs	161	1213 vs	160	cutoff

TABLE 17. *Assignments for $RbNO_3$ at liquid helium temperature for libration combinations*

Frequency	Separation from fundamental	Frequency	Separation from fundamental	Frequency	Separation from fundamental	Assignment
cm^{-1}	cm^{-1}	cm^{-1}	cm^{-1}	cm^{-1}	cm^{-1}	
726 ν_4		844 ν_2		1061 ν_1		ν_0
748	22	—		1084 vw	24	ν_0+L_1
780	54	—		1111 s	61	ν_0+2L_1
793 w	67	—		1126 s	65	ν_0+2L_2
—		920 m b	76	1140 s	80	ν_0+3L_1
—		—		1153 m	93	ν_0+3L_2
—		950 sh	106	1170 vw	110	ν_0+4L_1
—		964 m	120	1186 w	126	ν_0+4L_2
866 sh	140	988 s	144	1206 s	146	cutoff L_1
890 br	164	1005 s	161	—		ν_0+5L_2
≈901 b	175	1019 s	175	1232 s	172	cutoff L_2

The tabular data for $AgNO_3$ are not assigned. The complexity of the spectrum may be less than that of $TlNO_3$ and it seems that at least two librational modes are required. One peculiarity of the spectrum is the frequent appearance of triplet bands. One libration mode of 30 cm^{-1} with a cutoff of approximately 220 cm^{-1} appears reasonably certain.

Although the spectra of $CsNO_3$ and $RbNO_3$ appear to be similar, a somewhat different assignment can be given. A single libration mode of 30 cm^{-1} and a cutoff of 160 cm^{-1} is given for $CsNO_3$. A similar assignment for $RbNO_3$ is not obvious. Instead two modes one at 25 cm^{-1} and the other 30 cm^{-1} with barriers of 146 cm^{-1} and 175 cm^{-1} are indicated. However, it would appear that the 1153 cm^{-1} band might represent a cutoff not indicated by the assignment. Raman studies [36] show two frequency shifts of 109 cm^{-1} and 147 cm^{-1} for $RbNO_3$ both of which are observed in the spectra here. The 147 cm^{-1} band appears to correspond with one of the cutoff values.

e. Discussion of Raman and Infrared Assignments

The preceding analyses and assignments of the infrared spectra have been made with a minimum of reference to the considerable literature on the Raman spectra of the carbonates and nitrates (see Introduction). It may be noted that, so far as can be ascertained, the Raman shifts have never been assigned to a series of bands arising from librational motion of the anion about the trigonal axis. Some Raman bands have been assigned to libration perpendicular to this axis. Couture [10] pointed out that the fundamental libration used here should be inactive or at most weakly active in the Raman spectrum. However, analysis shows that the *combination* bands should be active in the infrared. It may be noted that no shift as low as 30 cm^{-1} has been reported in the Raman spectra of these materials but Krishnamurti [42] has recently reported that the few shifts obtained by routine Raman studies appear to consist of bands covering a wide frequency range when high resolution and long exposures are employed. He attributed the fine structure to superlattice vibrations.

In the present data the separations between the fundamental and the summation bands can be identified in part with a series of Raman shifts reported for the material of interest. The Raman assignments for these shifts involve individual translational and librational lattice modes. The evidence in favor of the librational assignment as opposed to the translational assignment and vice versa will be summarized here.

The effect of temperature on sum and difference bands of the fundamental ν_1 observed in many spectra represents good evidence that a very low lying frequency of the order 20 cm^{-1}–30 cm^{-1} is involved. The additional finding that this frequency represents the separation of a large number of bands in almost all spectra studied is considered to be significant. Furthermore, all structures, both carbonates and nitrates, yield a spectrum in which a frequency difference of the order of 20 cm^{-1}–30 cm^{-1} appears independent of the cation. The materials studied here contain one common factor—a planar anion having trigonal symmetry—and it appears that the recurring frequency difference should be attributed to this source. A librational motion of these anions all of which have essentially the same principal moments of inertia would be expected to occur at a frequency determined largely by the interionic potential forces. There is evidence that the anions are closely packed in these crystals [45, 77] and the interionic forces would be of the same general order of magnitude. It appears reasonable to conclude that the low frequency fundamental

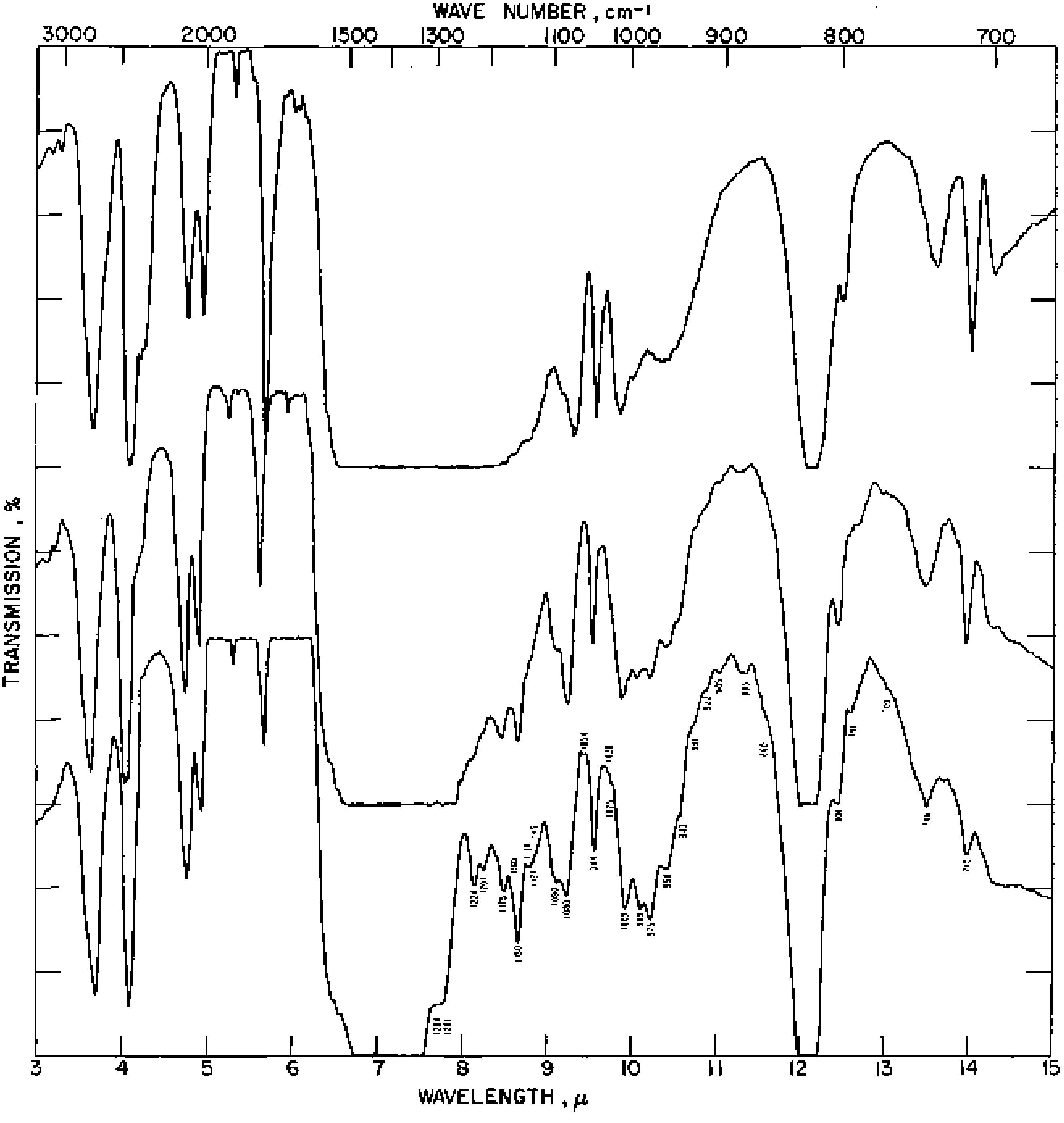

FIGURE 18. *Infrared absorption spectra of* TlNO$_3$ *at room temperature (top), liquid nitrogen temperature (center), and liquid helium temperature (bottom).*

arises from libration of the anions. The nature of the libration is not apparent and, as noted in the previous discussion, more than one frequency appears to be involved in some instances. However, based on the X-ray and neutron diffraction data previously cited which indicate libration about the trigonal axis, it is concluded that the libration responsible for the 20 cm^{-1}–30 cm^{-1} band spacing is a torsional oscillation about the trigonal axis.

Conversely, the bands observed here could be assigned to a large number of separate translational lattice modes in combination with the fundamentals. However, it seems unlikely that individual translational modes would have frequencies such as to yield a series of bands with uniform spacing. It is even more unlikely that similar series would be produced by such a variety of structures and cations. Therefore, the explanation that individual transla-

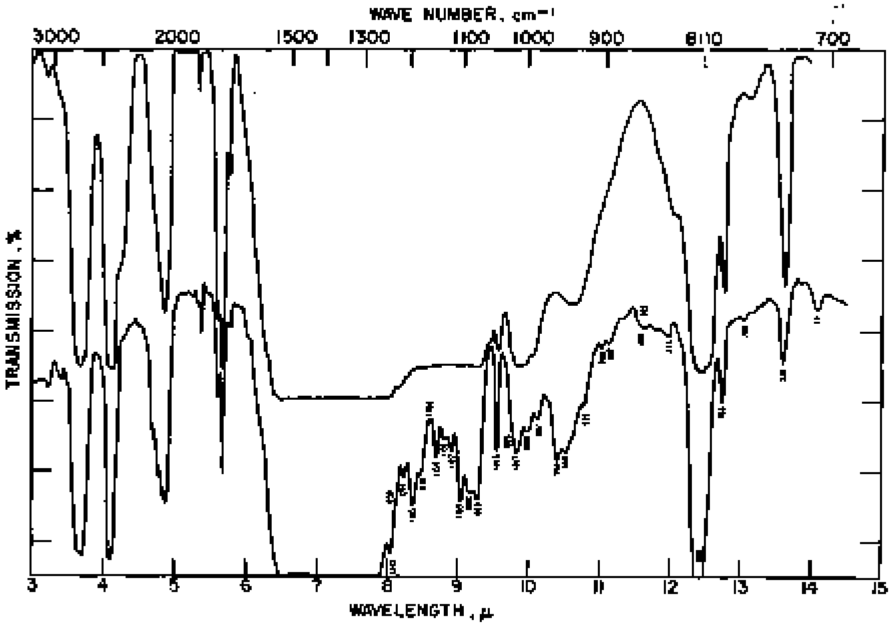

Figure 19. *Infrared absorption spectra of $AgNO_3$ at room temperature (top) and liquid helium temperature (bottom).*

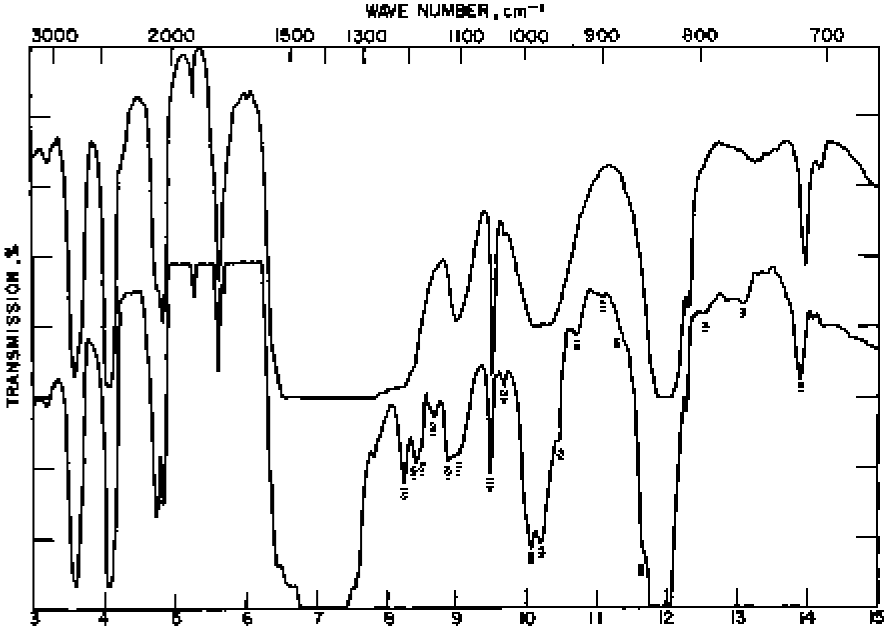

Figure 20. *Infrared absorption spectra of $CsNO_3$ at room temperature (top) and liquid helium temperature (bottom).*

tional modes are involved must be rejected. However, there remains the possibility that the bands arise from combinations between the fundamental and successive levels of a translational mode of frequency near 30 cm^{-1}. The relative insensitivity of the frequency to the crystal structure and the mass of the cation and the independent evidence for libration makes this interpretation appear doubtful. In addition the band limit or cutoff frequency which is of the same general order of magnitude in all these materials is readily understood in terms of libration. It can be explained with somewhat more difficulty for translation. It appears that the majority of evidence available at this time appears to favor the interpretation of the data in terms of libration. However, it must be emphasized that on the basis of the present evidence, a translational origin for the observed bands cannot be rejected unequivocally.

The effect of temperature on the frequency, intensity, and shape of the summation bands has been noted in the discussion. It is to be expected that the frequencies of the bands involving a lattice mode should be more temperature dependent than

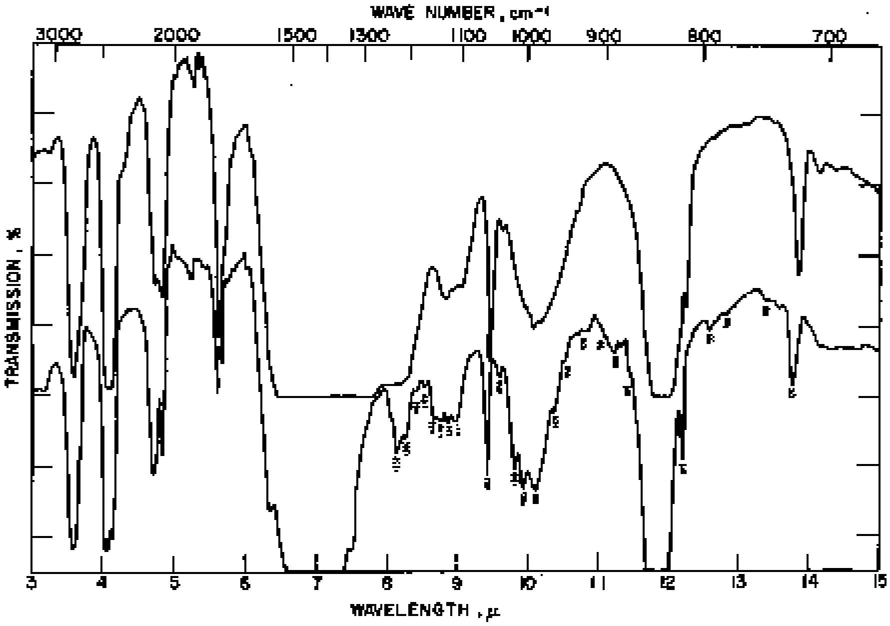

FIGURE 21. *Infrared absorption spectra of* $RbNO_3$ *at room temperature (top) and liquid helium temperature (bottom).*

the fundamentals. The lattice frequencies will depend on the interionic forces which are directly affected by the change in volume produced by cooling. If the forces are principally repulsive a shift to higher frequencies would be expected on cooling. This is actually observed. The fundamental internal frequencies have been shown to be rather insensitive to changes in volume. The intensity of the summation bands is expected to increase with decreasing temperature in these experiments. At ordinary temperatures, the higher librational levels are expected to be densely populated because of the low energy involved. As the temperature is lowered the lower levels increase in population at the expense of the higher levels. In absorption the intensity depends on the population of the lower of the two levels involved and, all other factors being equal, intensity should increase markedly as the lower levels become populated. Simultaneously it appears reasonable that the individual librational band widths should decrease.

Translational lattice modes must exist and no attempt has been made to identify these modes which would be active in combination with the fundamentals. However, in every spectrum there appear to be a few bands not falling into a regular sequence which might be assigned in this manner. There are also many unusually strong bands which might be attributed to superposition of a libration and translation combination with the fundamental. Such coincidences would be expected to be of frequent occurrence in a series of close spaced bands and might produce resonance splitting effects. Such splitting may produce the variation in spacing observed in some series of bands.

On the basis of the librational motion the cutoff frequencies are readily interpreted. According to Lander [45] the oxygen-oxygen interaction between neighboring anions defines the ordering. Spectroscopic data on the nitrates, carbonates, and borates [77] has also been interpreted in this manner. In a given crystal the anion should orient in the potential field in such a position that its oxygen atoms would be at a maximum distance from the neighboring oxygens. This position is not unique, however, as equivalent positions can be obtained by a rotation about the trigonal axis, potential minima being found every 120° or every 60° depending on the symmetry of the site. If sufficient energy is available a librating anion can surmount the energy barrier imposed by the repulsive forces of neighboring oxygen atoms and either rotate freely or, on losing energy, take up an equivalent position displaced by 120° or 60° from the original position. Therefore the librational bands should terminate at a frequency corresponding to the "free rotation" energy barrier.

No convincing arguments can be offered at this time for the intensity relationships in a series of bands. Hexter and Dows [35] have calculated that higher order combinations of the type postulated here should decrease in intensity exponentially. However, these calculations did not consider the interactions between neighboring ions. It appears reasonable to suppose that libration of the anion produces a change in the electronic charge distribution of the oxygen atoms. It appears likely that the perturbation of the charge distribution increases with increasing amplitude of the oscillation and should reach a maximum at the top of the barrier. What the effect of this change in charge distribution would be on the relative intensities is not clear so that this question cannot be answered at this time.

At the top of the energy barrier the librational modes change rapidly from a vibrational type to a rotational type. The intensity of transitions from a state corresponding to the ground vibrational level ($n=0$) and the ground librational level ($J=0$) to the upper vibrational level ($n=1$) and the upper rotational levels (say $J \geq 10$) would be very weak because such transitions are forbidden by rotational selection rules. Therefore if librational transitions below the top of the barrier have appreciable intensity because of electrical anharmonicity a rather sharp cutoff or band limit is indicated. Rotational transitions in addition to being forbidden would be expected to be very weak because of the absence of electrical anharmonicity in rotational motion.

f. Discussion of Libration and Energy Barrier Data

The observed data on libration frequencies and apparent energy barriers are tabulated in the first two columns of table 18. The libration frequencies listed correspond to maximum values observed for each substance, i.e., average values derived from the lower energy levels. Despite the wide variation in structure it is interesting to note that variations of the absolute values of libration frequency and energy barrier are relatively small. Libration frequencies appear to range from 15 cm^{-1} to 36 cm^{-1} and energy barriers from 140 cm^{-1} to 250 cm^{-1}. No reliable libration frequency was observed from $MgCO_3$ although the probable barrier is listed in table 18. The barriers tabulated represent the average estimates of the bands assigned as the three cutoff values of the three series of bands arising from combinations with ν_1, ν_2, and ν_4 which usually agree very well with each other.

Although qualitative arguments for libration have been presented in the previous section it remains to be demonstrated that the observed energy barriers are quantitatively of the correct order of magnitude. The following discussion will be limited to the calcite and cubic structures because of the uncertainties involved in the other structures. In addition only the data for $NaNO_3$ and $CaCO_3$ among the calcite structures will be considered because of doubts concerning the purity of the other materials. Column 3 of table 18 lists approximate anharmonicity corrections calculated from the observed frequencies for $CaCO_3$ (table 5), $NaNO_3$ (table 4), $Sr(NO_3)_2$ (table 13), $Ba(NO_3)_2$ (table 12), and $Pb(NO_3)_2$ (table 11). The anharmonicity corrections are observed to much larger for the calcite structures than for the cubic structures. This difference will be discussed subsequently. From the observed libration frequencies and the anharmonic corrections, the potential barrier for rotation may be calculated as follows.

TABLE 18. *Collected libration frequencies and energy barriers from infrared spectra at liquid helium temperature*

Material	Observed barrier [a]	Libration frequency, ν_L	Approximate anharmonicity correction	Calculated barrier [b]
	cm^{-1}	cm^{-1}	cm^{-1}	cm^{-1}
$MgCO_3$	220			
$CaCO_3$	152	36	1	162
$FeCO_3$	150	25?		
$MnCO_3$	160	25?		
$NaNO_3$	238	32	3	155
$Sr(NO_3)_2$	220	20	0.5	198
$Ba(NO_3)_2$	191	19	.5	179
$Pb(NO_3)_2$	167	18	.5	161
$TlNO_3$	250	25?		
$AgNO_3$	228	30?		
$CsNO_3$	161	25		
$RbNO_3$	176, 140	15, 20		

[a] Experimental values neglecting zero point energy. Approximate correction for zero point energy is $\nu_L/2$.

[b] Calculated barriers including correction for anharmonicity but neglecting correction for zero point energy. Approximate correction for zero point energy is $\nu_L/2$.

Assuming a rotational potential energy of the form

$$V=\frac{V_0}{2}(1-\cos n\theta) \tag{1}$$

where V_0 is the energy barrier, n the number of potential minima in a complete cycle, and θ the angular displacement from the equilibrium position, the potential barrier can be calculated from the libration frequency through the relationship

$$\nu_c=n\sqrt{\frac{V_0h}{8\pi^2cI}}. \tag{2}$$

In eq (2), ν_c corresponds to the corrected libration frequency, I the moment of inertia of the anion, and the other quantities have their usual significance. The corrected libration frequency is taken as equal to the observed libration frequency plus twice the anharmonic correction [33]. Taking the C—O and N—O bond lengths to be 1.25 A and 1.22 A, respectively, and independent of structure [80], the following two relationships for the potential barriers are obtained.

$$\text{for carbonates } V_0=4.26(\nu_c/n)^2. \tag{3}$$

$$\text{for nitrates } V_0=4.47(\nu_c/n)^2. \tag{4}$$

In calcite structures the anions occupy sites of symmetry D_3 and $n=6$. In the cubic structures the site symmetry is C_3 and $n=3$. Using eqs (3) and (4) and the corresponding data from table 18 the barriers were calculated and are given in column 4 of the table. The calculated barriers as tabulated have been corrected for the zero point energy contribution so as to be comparable with the observed values, that is the tabulated values represent the calculated barriers minus ½ the libration frequency.

A comparison of observed and calculated barriers shows that except for $NaNO_3$ the agreement is quite encouraging. Inasmuch as the libration frequencies cannot be determined with precision because of the width of the bands, and since a similar error exists in determining the cutoff frequencies, it is considered that the agreement between calculated and observed barriers is probably within the experimental error even in the case of $NaNO_3$. Furthermore the calculated barrier is dependent on the exact shape of the potential energy curve and on the bond distance used. The fact that the observed and calculated barriers are of the same order of magnitude supports the present interpretation of the observed spectra in terms of librational oscillations of anions that produce a series of bands terminating in a cutoff frequency which corresponds to the potential barrier for rotation.

The fact that the barriers are of the same order of magnitude implies that in these crystals the forces are of the same nature. This conclusion has been reached previously [77]. The smaller anharmonicity corrections of the cubic salts as compared with those of the calcites are to the expected. In the former there appear to be broader potential wells ($n=3$) than in the latter ($n=6$) and the levels are closer (20 cm^{-1} as compared to 30 cm^{-1}).

It will be noted that the agreement between calculated and observed barriers also implies that the assignments of the individual libration bands is essentially correct. If the data for $CsNO_3$ and $RbNO_3$ are used to calculate barriers it appears most likely that the nitrate ions must occupy sites of six-fold symmetry in these structures. However, similar calculations for $TlNO_3$ and $AgNO_3$ are not possible because of the great uncertainty in assigning the libration bands. From this point of view it is not surprising that the aragonite spectra is so complex because the anions occupy sites of symmetry C_s.

The absolute value of the potential barriers observed requires the conclusion that at ordinary temperatures, i.e., 300 °K, a considerable number of anions have energies in excess of the hindering rotational barrier. If large numbers of anions rotate, it is conceivable that the structure may become unstable. Several phase changes occur in the nitrates at moderate temperatures but the corresponding transitions in the carbonates take place only at relatively high temperatures [45]. There is no obvious correlation between the transition temperature and the height of the energy barrier. It must be concluded, therefore, that the cohesive energy of the crystal lattice is sufficient to accommodate considerable variation in the anion disorder and that the transitions are not caused primarily by the effect of the disordering. Since similar transitions in nitrates and carbonates are separated by several hundred degrees in temperature it appears that the cohesive energy, which is expected to be roughly four times as great in the carbonates, must largely determine the transition temperature. On the basis of the present interpretation most of the carbonate ions would have energies above the rotational energy barriers at temperatures well below the transition temperatures.

3.4. Overtones and Combinations of Fundamentals

Inspection of figures 1–21 for the carbonates and nitrates shows that numerous strong bands occur in the range 1700 cm^{-1} to 3000 cm^{-1}. The prism instrument provided insufficient dispersion and resolution for accurate study of this region. However, the number and strength of the bands indicate that free ion selection rules are not applicable in these crystals. In most spectra two sharp bands are observed, one near 1750 cm^{-1} and the other much weaker near 1800 cm^{-1}. Without exception these bands are located within a few wave numbers of the positions expected for the combinations $\nu_1+\nu_4$ and $\nu_1+\nu_2$, respectively. These bands can be assigned confidently. The other bands cannot.

For further study of this region several spectra were obtained on a grating spectrometer. The spectral regions from 1600 cm^{-1} to 4000 cm^{-1} for the liquid helium runs are given in figures 22, 23, 24, and 25 for $CaCO_3$, KNO_3, $BaCO_3$, and $Ba(NO_3)_2$ respectively. Frequencies of bands identifiable with certainty are listed in tables 19, 20, 21, and 22. The studies showed no appreciable shift of band positions in this region as the temperature was lowered although considerable sharpening of bands occurred at low temperature. Inspection of the spectra shows a very complex band system in this region and no assignments are given. It is particularly noted that in regions in which bands would be expected to correspond to the combinations $\nu_1+\nu_3$ and $2\nu_3$ the spectra show strong broad bands which appear to contain unresolved structure. Also of interest are the many bands appearing to contain shoulders extending more than 100 cm^{-1} to higher frequencies. Conversely similar shoulders are missing on the low frequency side. The spectra of KNO_3 and $Ba(NO_3)_2$ are particularly complex in this region. Several triple groups are evident in $Ba(NO_3)_2$ with components separated by about 30 cm^{-1} and 40 cm^{-1}. In general this region of the spectra does not offer any evidence to contradict the libration hypothesis and the complexity and broad bands would be expected if there is a libration-fundamental combination involved.

TABLE 19. *Overtones and fundamental combinations observed for calcite*

Frequencies	Frequencies	Fundamentals
cm^{-1}	cm^{-1}	cm^{-1}
3936 m	2798 m sh	ν_1—1070
3736 w	2560 vs	ν_2—881
3687 m	2490 s	ν_3—1407
3218 m	2320 mb	ν_4—712
3175 m	2210 mb	
2915 vs	2142 m	
	1960 m	

TABLE 20. *Overtones and fundamental combinations observed for* KNO_3

Frequencies	Frequencies	Fundamentals
cm^{-1}	cm^{-1}	cm^{-1}
3734 m shoulder to 3900	2396 s sh	ν_1—1051
3425 m shoulder to 3550	2360 m	ν_2—827
3108 w	2236 mb	ν_3—1420
3008 w	2150 mb	ν_4—714
2850 mb shoulder to 2970	2090 mb	
2782 mb	2060 m	
2733 m	1920 w	
2718 sh	1890 m	
2606 m	1873 ms ($\nu_1+\nu_2$)	
2560 mb shoulder to 2610	1762 s ($\nu_1+\nu_4$)	
2486 sh	1745 m	
2423 m		

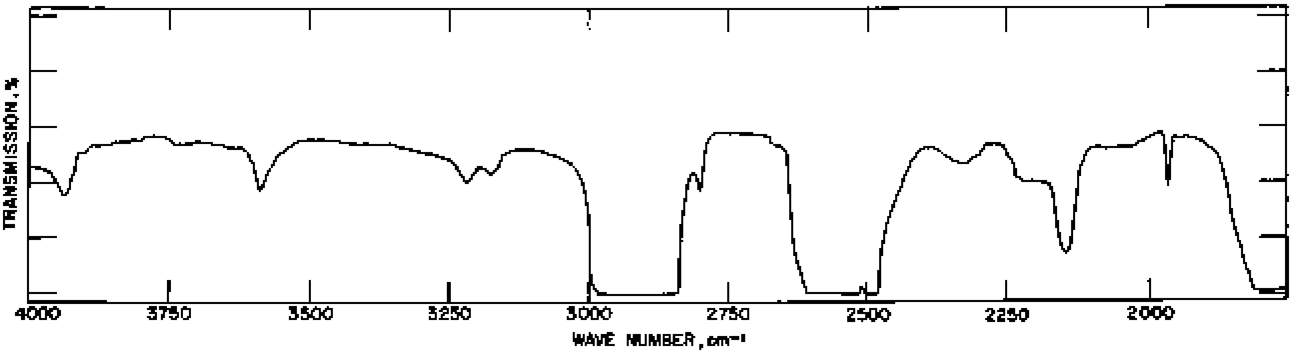

FIGURE 22. *Infrared absorption spectrum of* $CaCO_3$ *(calcite) at liquid helium temperature (1600 cm⁻¹ to 4000 cm⁻¹).*

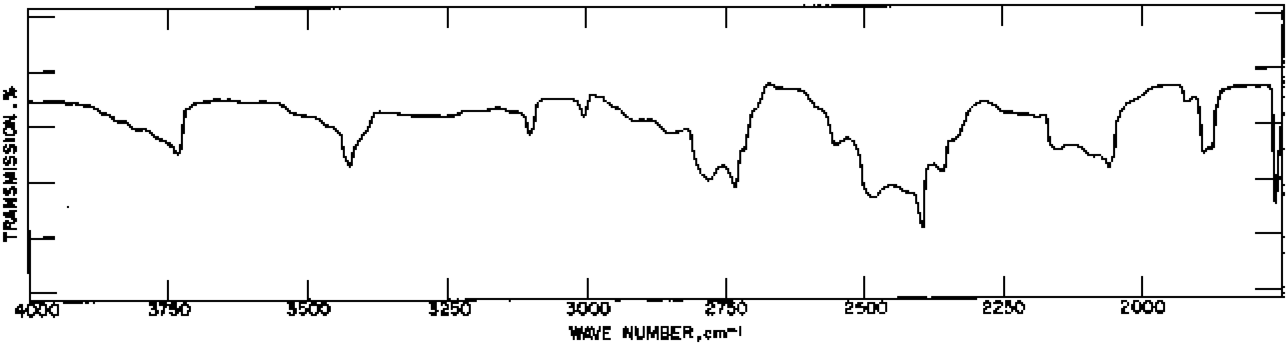

FIGURE 23. *Infrared absorption spectrum of* KNO_3 *at liquid helium temperature (1600 cm⁻¹ to 4000 cm⁻¹).*

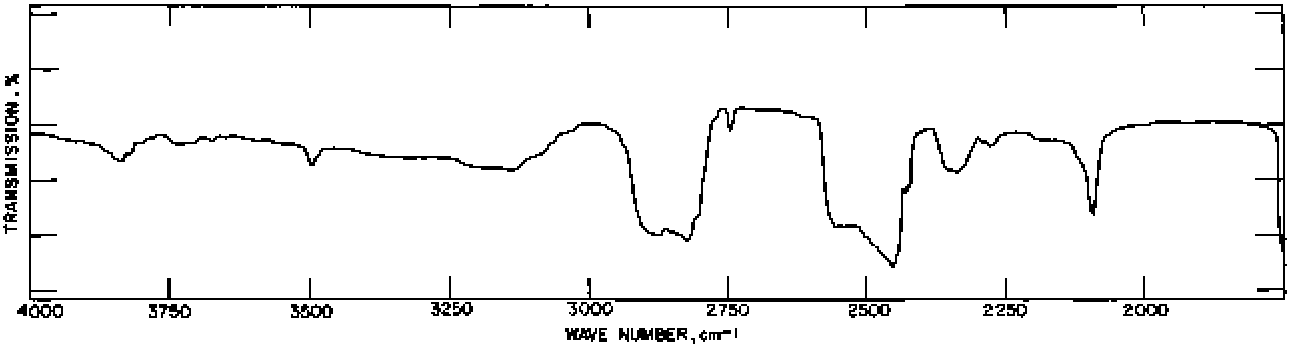

FIGURE 24. *Infrared absorption spectrum of* $BaCO_3$ *at liquid helium temperature (1600 cm⁻¹ to 4000 cm⁻¹).*

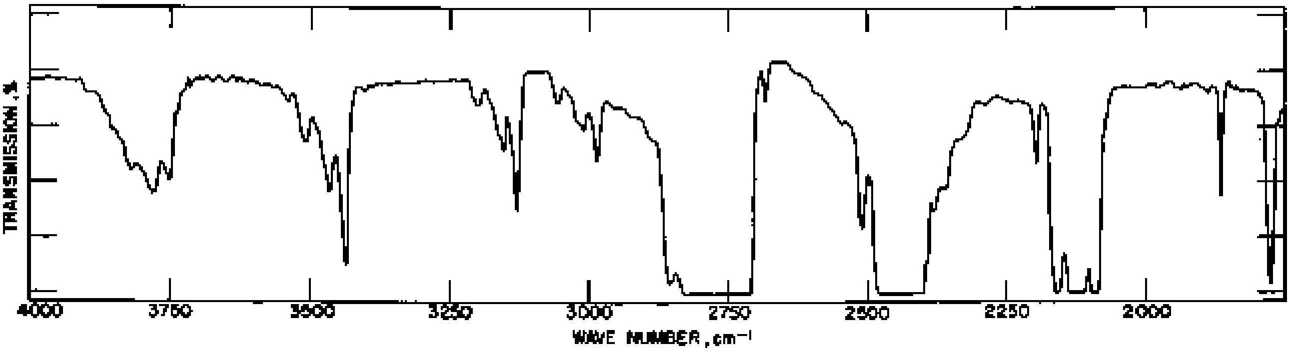

FIGURE 25. *Infrared absorption spectrum of* $Ba(NO_3)_2$ *at liquid helium temperature (1600 cm⁻¹ to 4000 cm⁻¹).*

TABLE 21. *Overtones and fundamental combinations observed for* $BaCO_3$

Frequencies	Frequencies	Fundamentals
cm^{-1}	cm^{-1}	cm^{-1}
2940 wb	2462 s	ν_1—1062
2898 w	2430 sb	ν_2—857
2880 sb	2423 sb	ν_3—1470
2820 b	2340 b	ν_4—702, 694
2805 sb	2062 sb	
2746 w	1755 sb ($\nu_1+\nu_4$)	
2550 sb	1749 s	
	1735 sb	

TABLE 22. *Overtones and fundamental combinations for* $Ba(NO_3)_2$

Frequencies	Frequencies	Fundamentals
cm^{-1}	cm^{-1}	cm^{-1}
3817	2653 m sh	ν_1—1052
3780 s	2550 b	ν_2—818
3750	2510 b	ν_3—1400?
3508	2440 b	ν_4—722
3485 s	2380 b	
3435	2360 b	
3200	2330 b	
3165 s	2290 b	
3128	2195 m	
3055	2156 vs	
3010 m	2120 vs	
2985	2090 s	
2885 w	1863 m ($\nu_1+\nu_2$)	
2855 s	1775 s ($\nu_1+\nu_4$)	
2770 vs	1620	

4. Conclusion

Infrared absorption spectra of inorganic nitrates and carbonates have been obtained on single crystals at room temperature, liquid nitrogen temperature, and liquid helium temperature. The diffuse absorption observed in the room temperature spectra between about 1400 cm^{-1} and 700 cm^{-1} is resolved at liquid helium temperature into a series of a large number of bands not attributable to fundamentals or combinations of fundamental frequencies of the anions. Most of these bands are readily interpreted as summation bands of fundamental frequencies with successive levels of a librating oscillator.

This interpretation is supported by the following, experimental observations:

1. The removal of the difference bands with reduction in temperature.
2. The large temperature dependence of the positions of individual bands as compared with that of the fundamentals.
3. The uniformity of the spacing of the individual bands within a given series of bands.
4. The similarity of the separation of the individual members of the separate series of bands from each of the fundamentals ν_1, ν_2, and ν_4.
5. The agreement in the separation of the band limits or cutoffs assigned from each of the fundamentals ν_1, ν_2, and ν_4.
6. The general similarity of the behavior in the vicinity of ν_3 with that observed at the other fundamentals, although the individual bands could not be distinguished.

The libration is considered to represent a planar torsional oscillation of the anion about the trigonal axis. The librational frequency appears to be dependent in part on the crystal structure and the ions involved. For a given material the librational frequency as determined from successive bands is reasonably constant. In the substances studied the librational frequency varied from about 15 cm^{-1} to 30 cm^{-1}.

Observed band limits in the spectra are interpreted as representing rotational energy barriers. These barriers are of the order of 200 cm^{-1} with the barrier height being dependent on the crystal structure and the ions involved. Barrier heights calculated from a cosine potential function agree reasonably well with the observed barriers for the cubic and calcite structures. Similar calculations have not been made for other structures studied because of doubtful assignments or unknown strucural details. In particular, the spectra of the aragonite structures are remarkable in detail and complexity and have not been analyzed successfully. However, the details of these and all other spectra studies appear to involve similar phenomena.

The question of whether this behavior is restricted to carbonates and nitrates cannot be answered fully. Preliminary studies on other salts at low temperatures indicates that similar band systems may exist. Further experiments are required to answer this question with certainty.

It is apparent that the band structure observed in these studies is not clearly seen in absorption spectra of thin films and polycrystalline specimens. In part, this may be due to the fact that it is customary in most instances to study specimens which do not absorb completely even in the strongest fundamentals and that the combination bands are too weak in comparison with the fundamentals to be observed under these circumstances. However, it would also appear likely that reduction of the crystal size below some minimum value as determined by the lattice mode might effectively eliminate the lattice mode and consequently the combination band. With lattice modes of low frequency the minimum crystal size might be readily attainable and preliminary investigations indicate some experimental evidence of a dimensional effect. Further study on these questions is under way.

The authors are indebted to L. Bolz for obtaining low temperature X-ray data.

5. Reference

[1] C. T. Anderson, J. Am. Chem. Soc. **56**, 340 (1934).
[2] C. T. Anderson, J. Am. Chem. Soc. **56**, 849 (1934).
[3] E. R. Andrew, J. Chem. Phys. **18**, 607 (1950).
[4] R. Bersohn and H. S. Gutowsky, J. Chem. Phys. **22**, 651 (1954).
[5] J. M. Bijvoet and J. A. A. Ketelaar, J. Am. Chem. Soc. **54**, 625 (1932).
[6] P. Chevin, W. C. Hamilton, and B. Post, American Crystallographic Assoc., Boulder, Colo. (July 31, 1961).
[7] M. Y. Colby and L. J. B. LaCoste, Z. Krist. **90**, 1 (1935).
[8] M. Y. Colby and L. J. B. LaCoste, Z. Krist. **84**, 299 (1933).

[9] L. Couture, Compt rend. **220,** 656 (1945).
[10] L. Couture and J. Mathieu, Ann. phys. **13,** 35 (1938).
[11] L. Couture and J. Mathieu, Compt. rend. **225,** 1140 (1947).
[12] L. Couture, Compt. rend. **220,** 87 (1945).
[13] L. Couture, J. Chem. Phys. **15,** 153 (1947).
[14] J. C. Decius, J. Chem. Phys. **23,** 1290 (1955).
[15] J. C. Decius, J. Chem. Phys. **22,** 1941 (1954).
[16] L. E. Drain, Faraday Soc. Discussions **19,** 200 (1955).
[17] D. A. Edwards, Z. Krist. **80,** 154 (1931).
[18] N. Elliott and J. Hastings, Acta Cryst. **14,** 1018 (1961).
[19] E. Ferrari, A. Sabatini, and P. Orioli, Gazz. chim. ital. **87,** 630 (1957).
[20] E. Ferrari, A. Sabatini, and P. Orioli, Ricerca sci. **27,** 1557 (1957).
[21] C. Finback and O. Hassel, J. Chem. Phys. **5,** 460 (1937).
[22] C. Finback and O. Hassel, Z. physik. Chem. **B35,** 25 (1937).
[23] J. Frenkel, Acta Physicochim. **3,** 23 (1935).
[24] L. Guilotto and G. Olivelli, J. Chem. Phys. **16,** 555 (1948).
[25] G. Glockler, Rev. Mod. Phys. **15,** 111 (1943).
[26] E. F. Gross and A. A. Shultin, Sov. Phys. Dokl. **2,** 371 (1957).
[27] P. Gunther, Ann. Physik **51,** 828 (1916).
[28] H. S. Gutowsky, G. E. Pake, and R. Bersohn, J. Chem. Phys. **22,** 643 (1954).
[29] C. Haas and J. A. A. Ketelaar, Physica **22,** 1286 (1956).
[30] R. S. Halford, J. Chem. Phys. **14,** 8 (1946).
[31] W. C. Hamilton, Acta Cryst. **10,** 103 (1957).
[32] S. B. Hendricks, E. Posnjak, and F. Kracek, J. Am. Chem. Soc. **54,** 2766 (1932).
[33] G. Herzberg, Molecular Spectra and Molecular Structure, Vol. II, Infrared and Raman Spectra of Polyatomic Molecules, 7th ed., p. 178 (D. Van Nostrand & Co., New York, N.Y., 1956).
[34] R. M. Hexter, Spectrochim. Acta **10,** 291 (1958).
[35] R. M. Hexter and D. A. Dows, J. Chem. Phys. **25,** 504 (1956).
[36] J. H. Hibben, The Raman Effect and its Chemical Applications (Reinhold Publ. Corp., New York, N.Y., 1939) pp. 428 and 445.
[37] R. M. Hinde and E. A. Kellett, Acta Cryst. **10,** 383 (1957).
[38] D. F. Hornig, J. Chem. Phys. **16,** 1063 (1948).
[39] J. Jaffray, Ann. phys. **3,** 5 (1948).
[40] J. A. A. Ketelaar and B. Strijk, Rec. trav. chim. **64,** 174 (1945).
[41] F. C. Kracek, T. F. W. Barth, and C. J. Ksanda, Phys. Rev. **40,** 1034 (1932).
[42] D. Krishnamurti, Proc. Indian Acad. Sci. **46A,** 183 (1957).
[43] D. Krishnamurti, Proc. Indian Acad. Sci. **43A,** 210 (1956).
[44] R. S. Krishnan, Proc. Indian Acad. Sci. **31A,** 435 (1950).
[45] J. J. Lander, J. Chem. Phys. **17,** 892 (1949).
[46] W. M. Latimer and J. E. Ahlberg, Z. physik. Chem. **148,** 464 (1930).
[47] W. M. Latimer and J. E. Ahlberg, J. Am. Chem. Soc. **54,** 1900 (1932).
[48] A. W. Lawson, Phys. Rev. **57,** 417 (1940).
[49] H. A. Levy and S. W. Peterson, Phys. Rev. **86,** 766 (1952).
[50] H. A. Levy and S. W. Peterson, J. Chem. Phys. **21,** 366 (1953).
[51] T. Liebisch and H. Reubens, Ber. Akad. Wiss. Berlin 198 (1919).
[52] J. Louisfert, Compt. rend. **241,** 940 (1955).
[53] G. Lutz, Z. Krist. **114,** 232 (1960).
[54] F. A. Mauer, Formation and Trapping of Free Radicals (Academic Press Inc., New York, N.Y., 1960) ch. 5.
[55] T. M. K. Nedungadi, Proc. Indian Acad. Sci. **14A,** 242 (1941).
[56] Nernst and Schwers, Ber. Akad. Wiss. Berlin 355 (1914).
[57] R. Newman and R. S. Halford, J. Chem. Phys. **18,** 1291 (1950).
[58] R. Newman and R. S. Halford, J. Chem. Phys. **18,** 1276 (1950).
[59] L. Pauling, Phys. Rev. **36,** 430 (1930).
[60] L. Pauling and J. Sherman, Z. Krist. **84,** 213 (1933).
[61] R. C. Plumb and D. F. Hornig, J. Chem. Phys. **21,** 366 (1953).
[62] A. K. Ramdas, Proc. Indian Acad. Sci. **37A,** 441 (1953).
[63] B. L. Rao, Proc. Indian Acad. Sci. **14A,** 48 (1941).
[64] B. S. R. Rao, Proc. Indian Acad. Sci. **19A,** 93 (1944).
[65] S. Satoh, J. Sci. Research Inst. **48,** 59 (1948).
[66] C. Schaefer, C. Bormuth, and F. Matossi, Zeit. f. Phys. **39,** 648 (1926).
[67] C. H. Shomate and K. K. Kelley, J. Am. Chem. Soc. **66,** 1490 (1944).
[68] L. A. Siegel, J. Chem. Phys. **17,** 1146 (1949).
[69] W. V. Smith, O. L. Brown, and K. S. Pitzer, J. Am. Chem. Soc. **59,** 1213 (1937).
[70] J. C. Southard and R. A. Nelson, J. Am. Chem. Soc. **55,** 4865 (1933).
[71] Standard X-Ray Diffraction Powder Patterns, NBS Circular 539, Vol. 1–6.
[72] C. C. Stephenson, L. A. Landers, and A. G. Cole, J. Chem. Phys. **20,** 1043 (1952).
[73] L. Vegard and L. Bilberg, Norske Videns. Akad. Oslo, 1931–1933.
[74] E. L. Wagner and D. F. Hornig, J. Chem. Phys. **18,** 296 (1950).
[75] E. L. Wagner and D. F. Hornig, J. Chem. Phys. **18,** 305 (1950).
[76] L. Waldbauer and D. C. McCann, J. Chem. Phys. **2,** 615 (1934).
[77] C. E. Weir and E. R. Lippincott, J. Research NBS, **65A,** 173 (1961).
[78] H. Winston and R. S. Halford, J. Chem. Phys. **17,** 607 (1949).
[79] R. W. G. Wyckoff, Am. J. Sci. **9,** 145 (1925).

(Paper 66A5–176)